The University of Southern Mississippi

The Aquila Digital Community

Summer 8-2014

Methane Dynamics in St. Louis Bay, Mississippi

Hannah Marie Roberts
University of Southern Mississippi

Follow this and additional works at: https://aquila.usm.edu/masters_theses

 Part of the Oceanography Commons

The University of Southern Mississippi

METHANE DYNAMICS IN ST. LOUIS BAY, MISSISSIPPI

by

Hannah Marie Roberts

A Thesis
Submitted to the Graduate School
of The University of Southern Mississippi
in Partial Fulfillment of the Requirements
for the Degree of Master of Science

Approved:

Dr. Alan Shiller
Director

Dr. Stephan Howden

Dr. Kevin Dillon

Dr. Maureen Ryan
Dean of the Graduate School

August 2014

ABSTRACT

METHANE DYNAMICS WITHIN ST. LOUIS BAY

by Hannah Marie Roberts

August 2014

A method of dissolved methane analysis was developed utilizing cavity ring-down spectroscopy and headspace equilibration. Samples of 70 mL were collected in 140 mL plastic syringes and equilibrated with a methane free headspace. Reproducibility was high (i.e. 4% typical RSD), and samples were successfully measured in the low nanomolar to high micromolar range. During method development, multiple research cruises were undertaken in the northern Gulf of Mexico. Stations included the Orca Basin, the Deepwater Horizon site, and the surrounding area. The Deepwater Horizon site showed no continuing leakage from October 2010 to June 2013. Samples collected from the northern Gulf of Mexico and the Orca Basin were in agreement with previous published work.

Using the new methodology, the methane dynamics of St. Louis Bay, MS was researched through a mass balance approach. The mass balance equations allowed simpler fluxes of the estuary to be measured, while complex fluxes were calculated. The total methane inventory of St. Louis Bay was found to vary between 900-7000 moles. The dominant sink was found to be air-sea flux, which varied between 4000-100,000 mol/day. River flux was found to be insignificant, ranging between 70-400 mol/day. The rate of air-sea flux prevented the river flux from affecting the interior of the estuary. Sediment flux remained as the only source of methane to the interior. Radon

measurements were collected to estimate the magnitude of the sediment flux; however,

concentrations were too low to be precisely measured.

ACKNOWLEDGMENTS

TABLE OF CONTENTS

LIST OF TABLES

Table

LIST OF ILLUSTRATIONS

Figure

CHAPTER I

INTRODUCTION

Methane

Methane is a greenhouse gas (GHG) that is produced by both natural and anthropogenic sources and plays a vital role in atmospheric chemistry (Kirschke et al., 2013; Solomon, 2007). Methane is oxidized within the troposphere by hydroxyl radicals, which can produce carbon monoxide, nitrogen dioxide, and hydroperoxide (Kirschke et al, 2013; Etheridge et al., 1992; Cicerone and Oremland 1988). Within the water column, methane is affected by chemical, biological, and physical variables and has been used as a natural tracer of groundwater inputs (Corbett et al., 1999).

This thesis addresses the issue of the estuarine flux of methane into the atmosphere. Specifically, I examined methane fluxes in a small, micro-tidal estuary as part of an effort to understand the role of estuaries in global methane dynamics. Estuarine fluxes into the atmosphere vary greatly among the limited studies available (Sebacher et al., 1986; Matthews and Fung, 1987; Cicerone and Oremland, 1988; Fung et al., 1991; Topp, 1991; de Angelis and Scranton, 1993; Thauer, 1998; Utsumi and Nojiri, 1998; Lu et al., 1999; Upstill-Goddard et al., 2000; Van der Nat and Middleburg, 2000; Purjava and Ramesh, 2001; Middleburg et al., 2002; Ding et al., 2003; Shalini et al, 2006; Borges and Abril, 2011; Kirschke et al., 2013; Steele et al, 2013). Important fluxes to each system vary with no outstanding pattern for all. However, these previous studies are limited in their application by the relatively small volume of published work. A large uncertainty in global estimations is inevitable due to this lack of data. As knowledge of methane dynamics within natural waters increases, a growing library of studies may

prove integral to understanding the magnitude of methane flux from estuaries. Similarly, important fluxes governing methane concentrations within estuaries are not exhaustively understood. For example, rates of methane oxidation have already proven to be sensitive to numerous factors, including methane concentrations (Utsumi and Nojiri, 1998; de Angelis and Scranton, 1993), salinity (Borges and Abril, 2011; de Angelis and Scanton, 1993), temperature (de Angelis and Scranton, 1993), light (Murase and Sugimoto, 2005), and sediment ecology (Boetius et al., 2000; Alperin and Reeburgh, 1985).

The St. Louis Bay (Mississippi) estuary presented a relatively simple model to study and was ideal for testing the idea of a mass balance approach. The shallow depth, wide interior and lack of stratification permitted the development of a simple box model. The elimination of more complex fluxes such as oxidation was possible, and the advantages of using this approach were best suited for such a system.

A new method of dissolved methane analysis in natural waters was developed as part of this research and is included in this thesis. As part of the work for developing and testing the new method, profiles of methane from several areas of the northern Gulf of Mexico were obtained, and I discuss those results here, too.

Sources of methane within the water column are both anthropogenic and natural, but are dominantly sourced to the decomposition of organic matter (Thauer, 1998; Kiene, 1991). Concentrations of dissolved methane in natural waters have previously been found to vary with organic matter content, oxygen availability, salinity, temperature, and wind velocity (Bange et al., 2006; Abril and Iversen, 2002; Kiene, 1991; Sebacher et al., 1986). High concentrations of methane are associated with low oxygen, high organic matter,

high stratification, and low mixing in the water column (Bange, 2006; Abril and Iversen, 2002; Kiene, 1991; Sebacher et al., 1986).

Freshwater, estuarine, and oceanic input of methane to the atmosphere is a complex process with limited observations that date back approximately 50 years (Reeburgh, 2007). Dissolved methane analysis requires two stages: extraction and analysis. Extraction techniques include adsorbing the gas onto a sorbent, freeze and trap methods, and headspace equilibration. Analysis was initially completed through manometric and microgasometric techniques (Reeburgh, 2007). Volumetric methods involve expanding a known amount of sample gas into a vessel containing a sorbent material (Battino and Clever, 1966). The gas becomes partially adsorbed onto the surface of the sorbent. Through the utilization of a mass balance, the gas adsorbed is calculated. A number of problems are associated with this technique (Battino and Clever, 1966). These include material purity, pressure, volume, and temperature measurement precision, leading to vast discrepancies in published data sets of known concentrations and solubility coefficients (Battino and Clever, 1966; Cook and Hanson, 1957).

Within the water column, dissolved methane is a non-conservative gas. Removal of methane from within estuarine and aquatic systems dominantly occurs by air-sea equilibration, physical gas transport, and oxidation by methanotrophs (Borges and Abril, 2011; Ding et al., 2003). Important methane fluxes into estuarine systems include fluvial inputs, methanogensis, ebullition, and submarine groundwater discharge (SGD) (Kiene, 1991).

Methane production is hypothesized to be the dominant source for many systems (Bugna et al., 1996; Marty, 1993; Kiene, 1991; Barnes and Goldberg, 1976). Methanogenesis occurs dominantly within anaerobic environments by methanogenic *Archaea* (Sowers, 2009). Anoxic sediments depleted in other electron acceptors but rich in organic matter permit the accumulation of high methane concentrations (Borges and Abril, 2011). Generally, suitable conditions occur lower in sediments where sulfate reducing bacteria do not outcompete methanogens (Kiene and Capone, 1988). Additionally, the diffusion of methane from sediments into the water column is likely prevented by anaerobic methanotrophic activity at the sulfate-methane boundary (Martens and Berner, 1977).

Sources of methane production within the water column are not exhaustively understood. However, internal portions of fecal pellets or the digestive tracts of certain species of zooplankton can create suitable environments for methanogens (de Angelis and Lee, 1994; Marty, 1993; Sieburth, 1991; Burke et al., 1983; Scranton and Brewer, 1977). Supersaturations of methane within surface waters are also observed to exist, with conflicting hypotheses as to their origins in either aerobic or anaerobic methane production (Metcalf et al, 2012; Karl et al., 2008; de Angelis and Lee, 1994; Marty, 1993; Sieburth, 1991; Burke et al., 1983; Scranton and Brewer, 1977). Anaerobic methane production would be sourced back to fecal pellets and gastrointestinal systems of various organisms (Burke et al., 1983; Marty, 1993; de Angelis and Lee, 1994). Others hypothesize different biological processes are driving surface water methane supersaturations (Scranton and Brewer, 1977; Sieburth, 1991; Karl et al., 2008; Metcalf et al., 2012).

Methane is also released from sediments through ebullition to the overlying water column or directly to the atmosphere (Borges and Abril, 2011; Bastviken et al., 2004; Ding et al., 2003; Topp and Hanson, 1991; Bartlett et al., 1987; Kipphut and Martens, 1982). Ebullition has been observed to be important in shallow estuarine systems (Klein, 2006; Bastviken et al., 2004; Martens and Klump, 1980). Bubbles are formed and forced upward through the sediment and water column after the partial pressures of dissolved gases exceed the hydrostatic pressure. As the bubbles rise from the sediments, pressure changes cause their partial dissolution in the water column before their release to the atmosphere (Borges and Abril, 2011). However, for most systems with reported rates of ebullition and sediment diffusive flux, diffusive fluxes dominate water column concentrations (Klein, 2006; Bastviken et al., 2004; Bugna et al., 1996). Additionally, diffusive fluxes are minor when compared to advection out of the sediments in coastal systems with substantial groundwater discharge (Santos et al., 2009; Burnett and Dulaiova, 2003; Bugna et al., 1996; Cable et al, 1996).

Fluvial sources supply large amounts of organic material, nutrients, gases, and fresh water (Kiene, 1991), creating favorable conditions for methanogenesis. Rivers and freshwater marshes exhibit these characteristics and are known methane sources to the atmosphere (Fung et al., 1991; Matthews and Fung, 1987; Sebacher et al., 1986)

The flux of methane between surface waters and the atmosphere is significant for many systems and is dependent upon multiple factors (Bange et al., 2006; Nouchi et al., 1994; Reeburgh et al., 1991; Sebacher et al., 1986). Wind velocity, air and water temperature, salinity, and concentrations within both reservoirs are factors controlling the

flux (Bange, 2006; Van der Nat et al., 2000; Sebacher et al., 1986; Baker-Blocker et al., 1977).

Oxidation by methanotrophs is hypothesized to be a significant sink of methane for some estuarine and freshwater systems (Borges and Abril, 2011; Abril and Iversen, 2002; Ding et al., 2003; de Angelis and Scranton, 1993; Kiene, 1991; Topp and Hanson, 1991). Methane oxidation can occur within both aerobic and anaerobic environments. Utsumi and Nojiri (1998) and Roslev and King (1995) found that peak rates of oxidation occurred at the transition zone between anoxic and oxic environments in freshwater systems. Factors found to affect aerobic and anaerobic methane oxidation rates in fresh and brackish waters include methane concentrations (Utsumi and Nojiri, 1998; de Angelis and Scranton, 1993), salinity (Borges and Abril, 2011; de Angelis and Scanton, 1993), temperature (de Angelis and Scranton, 1993) and light (Murase and Sugimoto, 2005). Significant factors found to affect methane oxidation within marine systems are sediment ecology (Boetius et al., 2000; Alperin and Reeburgh, 1985), physical characteristics of the water, and water mixing (Abril and Iversen, 2002; Kiene, 1991) as well as salinity (de Angelis and Scranton, 1993).

High salinity has been observed to inhibit methane oxidation. Oxidation has been found to account for 22-44% of the net CH_4 sink in freshwater, to 3% within brackish water and none within saline waters (Abril and Iversen, 2002; de Angelis and Scranton, 1993). Additionally, many methanotrophic organisms were not found to be active at ambient concentrations in sediments (Abril and Iversen, 2002). Sediments within brackish waters were found to uptake CH_4 (19-353 µmol/m^2/day), while sediments within saline waters were found to release CH_4 (3-400 µmol/m^2/day) (Abril and Iversen, 2002).

Radon, Radium, and Submarine Groundwater Discharge

Submarine groundwater discharge (SGD) is a source of water to the coastal ocean, driven by climatologic, hydrogeologic, and oceanographic processes. SGD includes both freshwater input and recirculated seawater and occurs via diffusion, localized springs, and advective flow. It is a pervasive coastal process that occurs within aquifers connected with the open ocean through permeable rocks or bottom sediments and when the head is above sea level (Johannes, 1980). Groundwater flows of sulfate-depleted freshwater favors methanogenesis (Albert et al., 1998). Upon mixing with coastal waters, this SGD becomes a flux of methane into the system.

SGD can be traced in a marine environment using methane, radium-226, and radon-222 as indicators of flow (Burnett and Dulaiova, 2003; Kim and Hwang, 2002; Corbettet al., 1999; Hussain et al., 1999; Bugna et al., 1996; Cable et al, 1996). Alternatively, SGD flow, radium, and radon concentrations can be used to measure the flux of methane from this source. The water column inventory of radon can be affected by in situ radium-226 decay, benthic diffusive-advective exchange, porosity of the sediments, water column decay, eddy diffusion along and across the pycnocline, and air-sea exchange (Burnett and Dulaiova, 2003; Bugna et al., 1996; Cable et al., 1996). In this case, eddy diffusion along and across the pycnocline can be neglected due to the size and well-mixed nature of St. Louis Bay. Diffuse, patchy seepage has been shown to be the greatest source of CH_4 to coastal systems (Santos et al., 2009; Burnett and Dulaiova, 2003; Bugna et al., 1996; Cable et al, 1996).

St. Louis Bay

St. Louis Bay, MS was chosen as an ideal study location. The estuary has the

potential to have the sources identified within the introduction. Additionally, the USGS

has placed a discharge gauging station on one of the fluvial sources, which is helpful for

estimating the fluvial flux into the estuary. It is also in close proximity to the lab,

allowing for minimal time between sample collection and analysis.

St. Louis Bay is a classic drowned river valley estuary with an approximately 3

km wide mouth to the Mississippi Sound. The climate is sub-tropical. The estuary has

approximately 4,000 hecatres of surface area with an average depth of 1.3 m, giving a

volume of approximately 5.2×10^7 m^3 (Eleuterius, 1984). It is vertically well mixed and

microtidal.

Two rivers empty into the estuary, the Wolf and the Jourdan Rivers in the

northeast and northwest, respectively. Flow from the two rivers averages 23.5 m^3/s and

20.0 m^3/s, but variability is high (Eleuterius, 1984).

Environments within the estuary include extensive marshes along much of its

shores with sand pumped onto limited portions of the western shore. Additionally,

seawalls extend for most of the western shore from the Waveland Yacht Club to the

Jourdan River. Sediments are mostly fine to very fine, with some patches of sand (Bera,

2014).

Biological composition in the interior of the estuary does not vary spatially

(Phelps, 1999). St. Louis Bay is a system which can be disrupted during instances of

higher freshwater input from land sources; however, the benthic community is

hypothesized to have adapted to such episodic events (Phelps, 1999; Pearson and

Rosenburg, 1978).

Hypotheses

The hypotheses for the study are presented as follows: 1) St. Louis Bay is a net

source of methane to the atmosphere, 2) sediment flux is the dominant source of methane

to the estuary, 3) oxidation is a significant sink of methane to the system, and 4) methane

concentrations are highest in warmer months when storms are less frequent.

CHAPTER II

REVIEW OF RELATED LITERATURE

Dissolved methane research has been relatively limited in scope and volume of data. Historical and modern techniques require complex and time consuming lab analysis (Reeburgh, 2007; Kolb and Ettre, 2006; Battino and Clever, 1966). The development of a new method was necessary to expedite data collection to reflect the dynamic nature of this gas.

Modern techniques often utilize gas chromatographs (GC) that require multiple steps for sample preparation before analysis (Kolb and Ettre, 2006; Battino and Clever, 1966). Gas chromatography was introduced in the early 1950's (Reeburgh, 2007). A liquid is supported in a column while a carrier gas continually bathes the liquid. Equilibrium is established between the two phases. A second gas (or vapor) is transported by the carrier gas to be partitioned between the gas and liquid (Battino and Clever, 1966).

Hydrocarbons were originally analyzed with GC analysis through the addition of freeze-trap methods, where hydrocarbons are stripped from solution (Swinnerton and Linnenbom, 1967; Battino and Clever, 1966). After freezing, the gas is then re-warmed and introduced through a sample loop to a gas chromatograph (Swinnerton and Linnenbom, 1967).

Recent techniques dominantly utilize headspace equilibration alongside gas chromatography (Reeburgh, 2007; McAuliffe, 1963). A known volume of liquid in a closed container is mixed with a headspace of gas until equilibrium is reached (Kolb and Ettre, 2006; Ioffe and Vitenberg, 1984). By extracting a known volume of headspace, the actual concentration can be calculated using established solubility constants. In addition to the static liquid GC method described above, dynamic headspace sampling, solid-

phase microextraction (SPME), and multiple headspace extraction (MHE) have been introduced in recent years (Kolb and Ettre, 2006). SPME is used in conjunction with classic headspace techniques by either immersing a coated fiber in a liquid sample or sampling the headspace above a liquid or solid sample (Kolb and Ettre, 2006). The classic approach and SPME house the headspace in a closed vial, while the dynamic sampling procedure uses exhaustive gas extraction (Kolb and Ettre, 2006). The procedure of MHE also utilizes exhaustive gas extraction, but it is carried out in concurrent samplings, rather than a continuous process (Kolb and Ettre, 2006). Multiple headspace extraction allows for an easier calibration process and provides data to show linearity and precision of a determination (Kolb and Ettre, 2006).

Gas chromatography techniques involve multiple requirements and assumptions (Battino and Clever, 1966). First, liquids are restricted to those with high boiling points. Second, steady states and transient equilibriums are part of the process as the carried component travels through the column. Third, the concentration of the carrier gas is lowered by the addition of the third component to the system. Fourth, the partial pressure of the third component is difficult to ascertain as the concentration within the re-warmed sample not likely to be homogenous throughout. However, GC methods are low cost, fast, and have a reproducibility typically near $\pm 3\%$ (Battino and Clever, 1966).

The method introduced in this paper utilizes headspace equilibration and cavity ring-down spectroscopy (CRDS). Through the use of a Picarro G2301 CRDS analyzer, rapid CH_4 measurements are performed with less than 10% of the relative standard deviation. The CRDS uses a single-frequency laser diode and a cigar-shaped laser cavity defined by three mirrors (Crosson, 2008). This apparatus provides an effective path

length of many kilometers, enabling the ability to measure trace gases from air samples (Crosson, 2008). The CRDS measures light absorption by determining light intensity decay within the cavity over time (ring-down time) (Crosson, 2008). Non-target gas species are eliminated by comparing ring-down times between cavities with and without target gases and by tuning the laser wavelength (Crosson, 2008). The CRDS then calculates continuous ppm concentrations of CO_2, CH_4, and water vapor using formulae by Busch and Busch (1999).

Previous work with CRDS technology has proven fruitful in many regards to atmospheric and dissolved gases (Becker et al., 2012; Yvon-Lewis et al., 2011; Alexander, 2006; Hallock et al., 2002). Becker et al. (2012) and Yvon-Lewis et al. (2011) used headspace analysis for continuous measurement of dissolved gases. Warner et al. (2013) previously utilized discrete sampling with the CRDS technology similar to the method described below. However, a much larger sample of 900 mL was used. This volume of sample requires additional time for collection and is less than ideal on open ocean research cruises. The method described below eliminates these issues by taking smaller samples while maintaining a high level of precision. Additionally, the method by Warner et al. (2013) was developed for measuring the high µM concentrations found in groundwater. Their method was unable to precisely measure the low nM concentrations typical of oceanic and estuarine waters. The method provided below results in a wider range of methane concentrations measured with greater accuracy and precision in the nM range.

CHAPTER III

METHODOLOGY

The CRDS instrument used in this work was a Picarro, Inc. (Santa Clara, CA) G2301 CO_2, CH_4, H_2O analyzer. The instrument can measure CH_4 in air in the 0-20 ppm range, though instrumental specifications (e.g., drift <3 ppb over 1 month) are only guaranteed in the 1-5 ppm range. The research instrument was modified with an additional extended range mode for determining CH_4 up to 1000 ppm.

For headspace equilibration of natural water samples, 140 mL Monoject™plastic syringes (Kendall Healthcare) fitted with 3-way luer lock valves (Cole-Parmer) were filled with 70 mL sample water and 70 mL of methane-free zero air. This volume of water sample was only altered when methane concentrations exceeded the detection limits of the Picarro G2301 CRDS analyzer. Note that at least ~70 mL of headspace is required in order to obtain a precise result with the G2301. To minimize bubble accumulation within the syringes, approximately 50 mL of sample was initially introduced into the syringe. The syringe was tapped to gather all air bubbles toward the valve. A small amount of ambient air was then introduced while keeping the syringe upright. The air and water were then carefully expelled from the syringe, and the rinsing/bubble elimination was repeated twice more before collecting the desired sample volume (70 mL for the experiments reported below). Valves were dried fully and a volume of methane-free zero air (70 mL for the experiments herein) was added to each sample. Pressure disequilibrium within the sample syringe was alleviated by briefly opening the 3-way valve after disconnecting it from the cylinder of zero air. A preliminary test suggested that dissolved methane equilibrates with the headspace with a minute or less of vigorous shaking. However, it was desired to have the samples close to

room temperature (or at least a known, measured temperature) in order to be able to correctly calculate the methane solubility. Therefore, samples were placed on a shaker table for typically 30 minutes. This time was extended if the temperature of the sample was not close to that of the lab air; however, the exact temperature at equilibration is not necessary as methane solubility is not strongly affected by temperature (Wiesenburg and Guinasso, 1979).

After sample-zero air equilibration, the equilibrated headspace of each sample was transferred to a clean, dry syringe to minimize the possibility of an accidental introduction of water into the CRDS. The transfer procedure included a brief "rinsing" of the valve pathway between the two syringes using a little of the headspace gas. Valves and the interior of each transfer syringe were checked to ensure no water was also transferred. The headspace was then drawn into the Picarro G2301 CRDS analyzer by the analyzer's pump. A procedural blank is made by transferring 70 mL of zero air between two syringes before measurement. The blank value was equivalent to a ~0.06 nM concentration of dissolved CH_4. The measurement of CH_4 is the "wet" air measurement given by the G2301 since published solubility relationships are based on water-saturated air, and it is assumed that our equilibration process saturates the headspace with water vapor.

Dissolved concentrations of methane were calculated from headspace concentrations via the solubility equation of Wiesenburg and Guinasso (1979) (1) and Henry's Law (2).

$$C^* = \exp[\ln((pCH_4 \times 10^{-6})) + A_1 + A_2\frac{T}{100} + A_3\ln(\frac{T}{100}) + A_4\frac{T}{100} + S^*\left\{B_1 + B_2\frac{T}{100} + B_3\frac{T}{100}^2\right\}] \ (1)$$

$$K_h = \frac{C^* \times 10^{-9}}{pCH_4 \times 10^{-6}}$$

(2)

$$\text{CH}_4 \text{ (nM)} = \left[(pCH_4 - pCH_4^B)10^{-6} \times \left(K_h + \frac{\frac{V_{head}}{V_{water}}}{RT} \right) - \left(pCH_4^{Init} \times 10^{-6} \right) \times \frac{\frac{V_{head}}{V_{water}}}{RT} \right] 10^9$$

(3)

The pCH_4 is the concentration (ppm) of methane in the equilibrated headspace, pCH_4^B is the methane measurement of the procedural blank, pCH_4^{Init} is the initial methane concentration of the equilibration gas (generally very close to zero for zero air), and C^* is the dissolved concentration of methane in equilibrium with pCH_4 at temperature T (K) and salinity S. The constants A_1, A_2, A_3, A_4, A_4, B_1, B_2 and B_3 are given by Wiesenburg and Guinasso (1979). The volumes of the headspace and water sample are V_{head} and V_{water}, respectively, and R is the gas constant. Equation (3) is thus derived from a mass balance on methane in the equilibrated headspace and water sample, accounting for procedural blanks and any methane initially in the headspace.

Method Assessment

The reproducibility of the method was tested using tap water and 140 mL syringes. Sample water was added to multiple syringes and allowed to equilibrate on a shaker table for varying times. Relative standard deviations were below 8% (see Table 1). Samples deviating the most from the average concentration did not correlate with the time on the shaker table.

Table 1

Relative standard deviations for tap water and field samples with n repetitions. Different concentrations of methane were achieved by bubbling air through a carboy filled with water for varying amounts of time.

Date	Number of replicates	Time on Shaker Table (minutes)	Average CH_4 (nM)	Relative Standard Deviation
June 29 2011	20	10-60	607	2.3%
June 30 2011	10	10-120	594	1.7%
July 6 2011	12	10-150	484	5.7%
July 7 2011	12	10-120	373	5.1%
January 31 2013	3	15	248	3.5%
January 31 2013	6	15	175	6.3%
January 31 2013	5	15	31	5.1%
July 18, 2011	8	60	4	8.3%

The research version of the G2301 has two measurement modes. The first mode measures methane within a low range (LR) at concentrations up to 5 ppm. This configuration comes standard with the G2301. The second mode measures high methane concentrations (HM) between 5 ppm and 1000 ppm. Both modes were tested with a known methane gas concentration of 4.86 ppm (±1%) over a period of 5 minutes of continuous flow. HM reported a concentration of 4.97 ppm (±2.6%) while LR reported a concentration of 4.93 ppm (±0.06%). The relative standard deviation between the two modes was 0.5%, and the measured value for the LR mode was 1.4% higher than the calibrated value of the gas.

Drift within the CRDS is minimized by actively stabilizing temperature and pressure within the cavity. Laser wavelength, sample pressure, and temperature are all

controlled, which contribute to a typical drift of ppbv levels over 30 days according to instrument specification). Drift correction is recommended by Picarro every year. However, measurements of a tank of breathing air (1.9 ppm CH_4) and zero air (0 ppm CH_4) showed no noticeable drift over the course of two years, with a relative standard deviation between the two years less than the variance on a given day (±0.001 ppm CH_4).

A test of the linearity and precision of low ppm/ppb measurements of CH_4 was completed (see Figure 1). Headspace equilibration of samples with low nM concentrations of dissolved methane yielded concentrations within the headspace less than 0.1 ppm. The manufacturer certified the instrument to 0.5 ppb CH_4; however, commercial standards were not available for a test of the instrument's calibration at the low CH_4 partial pressures observed with our method. Therefore, standards were mixed in the lab using two known gases: breathing air (1.9 ppm) diluted with zero air (0 ppm). For concentrations greater than 10% breathing air, a sample syringe (SS) was filled to a specified volume of breathing air after rinsing five times with breathing air gas. A transfer syringe (TS) was then filled with zero air also after rinsing five times with zero air and connected to the SS. The TS was opened, and a small amount of zero air was used to clear the connected valves and to equalize the pressure within the syringe. The SS was opened, and the appropriate amount of zero air was added to the SS. When gases were transferred between syringes, the volume within the syringe was adjusted according to the known volume added to the syringe to ensure pressure equilibration. The SS was left to equilibrate for an hour.

For concentrations less than 10% breathing air, a 500 mL Tedlar® EconoGrab™ gas bag (Zefon International) was filled with zero air and breathing air to make an

approximately 10% mixture of breathing air in zero air. Prior to equilibrating, the bag

was filled with zero air, and a vacuum was then used to remove all air. The process of

filling and evacuating was repeated three times, ending with a vacuumed gas bag with

minimal air or CH_4. Syringes were then used to transfer proportional amounts of each gas

to the bag. Table 2 lists volumes of gas used for each measurement. With each

consecutive addition, the syringe was rinsed five times with zero air or breathing air and

then filled with the corresponding gas to the correct volume. A small volume of gas from

the syringe was then used to clear the connection between the syringe and bag before

adding the appropriate amount of gas. The gas bag presented negligible resistance to

inflation, so pressure equilibration was not an issue. The bag was left to equilibrate for 15

minutes. The gas bag was then used as a reservoir of gas to be measured. For each

measurement, a small amount of gas from the bag was used to clear the connection

between the bag and syringe. A volume of 70 mL of gas from the bag was added to the

syringe through the use of the syringe plunger to avoid pressure disequilibration and was

then measured using the CRDS.
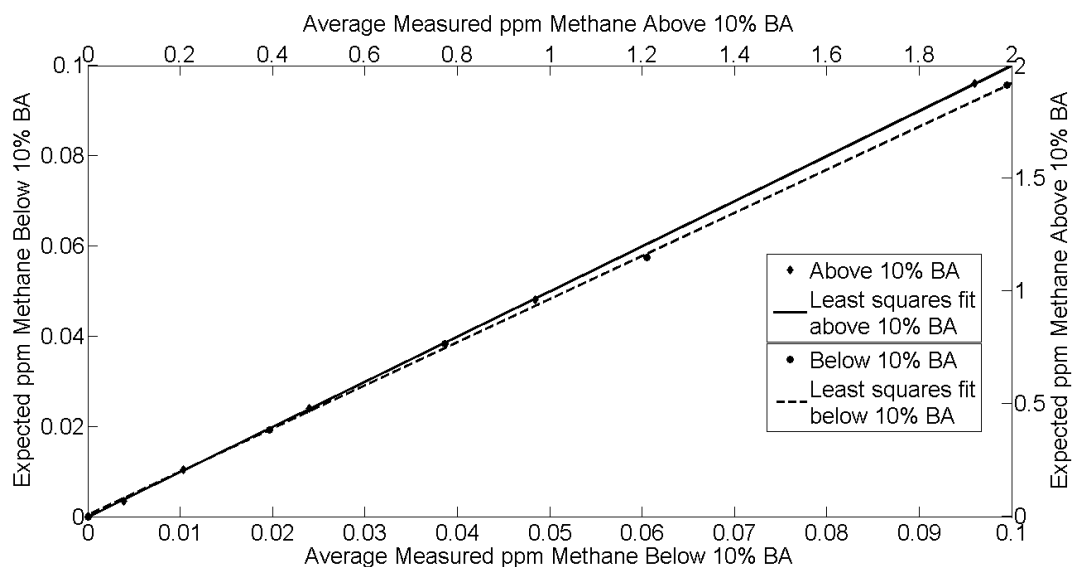
Figure 1. Linearity test of the Picarro G2301 CRDS analyzer. Two methods of gas dilution (see text) were used. The r^2 value for above 10% breathing air is 1.001, and the value for below 10% breathing air is 0.956.

Results showed a slope of 1.001 for measurements greater than 10% and 0.956 for measurements less than 10%. Correlation coefficients for these data are 0.9998 and 0.99998, respectively. ANCOVA analysis of the data shows a p-value of 1. This experiment shows the linearity of the G2301's calibration at low concentrations between the zero air blank and the calibration gas.

Incubations were conducted in triplicate with samples from station 14 to approximate the net oxidation of methane in the water column (i.e., oxidation minus production) and to check the calculations of the mass balance. Syringes were filled as described above for discrete sampling and analyzed at varying time intervals between 0 and 24 hours (Utsumi and Norjiri, 1998). During incubation, syringes were stored in an incubator at a constant temperature of 29.9°C. This temperature was pre-set for other experiments within the incubator. Each analysis was completed in duplicate.

Radon samples were collected in bottom waters at a central location and analyzed using the methods of Lee and Kim (2006) as modified by Burnett et al. (2001). Water samples were collected using tubing and a peristaltic pump. The samples were stored in 2 L cleaned soda bottles until analysis by a radon-in-air monitor (RAD-7; Durridge Co.). Each sample bottle was filled from the bottom up and allowed to overflow at least three times before capping immediately following removal of the water tubing. When a sample was analyzed, 50 mL of water was removed, and a multi-port cap was placed immediately on top. The sample was connected to the RAD-7 in closed air-loop mode with a desiccant column for 2 hours per sample. The activity of the ^{222}Rn was then counted from its alpha-emitting daughters. The lab procedure was repeated in two weeks to measure ^{226}Ra. The two-week period allowed for the decay of the initial ^{222}Rn and the achievement of radioactive steady state between the parent ^{226}Ra and newly ingrown ^{222}Rn.

Figure 2. St. Louis Bay sampling stations.

Table 2

Station locations.

Station	Latitude Degrees, Decimal Minutes	Longitude Degrees, Decimal Minutes
1	30 19.854	89 19.569
2	30 20.501	89 19.809
3	30 20.631	89 21.163
4	30 20.128	89 23.030
5	30 20.702	89 22.226
6	30 21.257	89 20.986
7	30 21.749	89 21.270
8	30 21.138	89 20.134
9	30 22.224	89 18.964
10	30 21.382	89 19.889
11	30 21.515	89 18.833
12	30 21.519	89 17.307
13	30 21.530	89 17.589
14	30 20.912	89 18.660
15	30 20.513	89 18.470
16	30 20.494	89 17.160
17	30 20.524	89 16.162
18	30 19.868	89 17.650
19	30 19.881	89 18.51
20	30 18.777	89 18.428

Stations were chosen to represent the potential fluxes in St. Louis Bay (see Table 2 and Figure 2). Stations 4 and 12 represent the Wolf and Jourdan Rivers. Stations 6, 10, 14, and 15 are representative of the central area of the estuary. Station 20 represents the mouth to the coastal ocean.

Methane samples were collected from each of the 20 stations. Radon-222 and radium-226 samples were collected at station 14 and taken in triplicate. Ambient air samples and incubation samples were taken at station 14. Salinity, temperature, and weather conditions were recorded at each station.

Preliminary field work showed methane concentrations ranging from 30 – 375 nM in January 2013. High concentrations were observed within the rivers with the lowest concentrations observed in the center of the estuary. Further preliminary field work was conducted to determine if surface and bottom water samples for methane were necessary.

CHAPTER IV

ANALYSIS OF DATA

There was no difference between surface and bottom water methane

concentrations in St. Louis Bay, with differences between measurements less than or

equal to differences between duplicates (see Table 3).

Table 3

Surface and bottom water comparisons of Saint Louis Bay, MS. Stations 1-2 were collected January 31, 2013. Station 1 was located toward the center of the estuary towards the mouth, station 2 was located just outside of a marsh on the eastern side of the estuary. Stations 3-6 were collected July 11, 2013 in the marshes in the east, northeast and north, respectively.

Station	n	Depth	Average nM Concentration	Average of Surface/Bottom Waters
1	3	Surface	30	32
1	3	Bottom	34	
2	3	Surface	175	175
2	3	Bottom	175	
3	1	Surface	466	457
3	1	Bottom	447	
4	1	Surface	527	530
4	1	Bottom	532	
5	1	Surface	753	775
5	1	Bottom	795	

Sampling was completed in both cooler and warmer months with varying

environmental conditions (see Table 4). Temperature, wind direction, wind velocity, and

tide amplitude were collected from the National Weather Service. Water residence time

was calculated using the tidal prism and the approximate water volume in the estuary (see

Calculations).

Table 4

Environmental parameters on sampling dates. Air temperature, wind speed, wind direction and tidal data were used from the National Weather Service. Water residence time was calculated by dividing the volume of St. Louis Bay by the tidal prism (See Calculations).

Date	Sampling Time	Temp (C)	Wind (m/s)	Wind Direction	High Tide Time	High Tide with Respect to MLLW (m)	Low Tide Time	Low Tide with Respect to MLLW (m)	Water Residence Time (days)
8/1/2013	9:00-12:0	29	2.2	NW	8:40 AM	0.53	8:57 PM	0.02	3
9/23/2013	9:30-11:3	25	2.7	E	1:56 AM	0.6	11:22 AM	0.17	4
9/30/2013	9:00-11:0	24	2.2	E	8:30 AM	0.49	7:20 PM	0.2	6
10/8/2013	9:30-11:3	19	2.2	N	1:40 AM	0.66	11:25 AM	0.11	3
10/29/2013	9:00-11:0	21	0.89	ESE	7:15 AM	0.38	5:02 PM	0.26	7
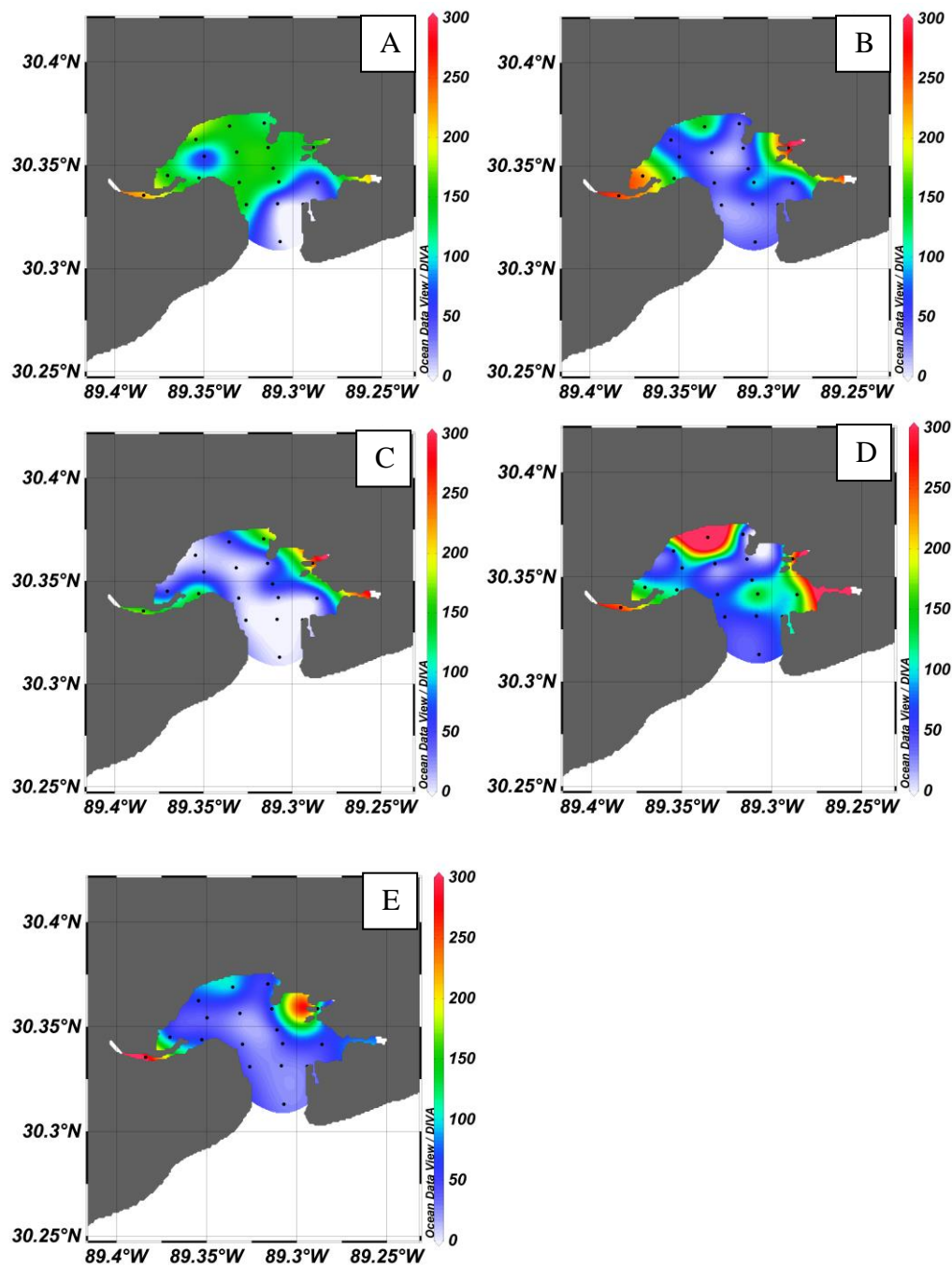
Figure 3. Methane (nM) sampling results using Ocean Data View DIVA gridding. Sampling Dates from August 1, 2013 (A); September 23, 2013 (B); September 30, 2013 (C); October 8, 2013 (D); October 29, 2013 (E).

Some higher concentrations were observed around station 14 (see Figure 3 or Table A-1). For all stations, methane concentrations ranged between 0-599 nM, salinity ranged between 1-17.9, and water temperature ranged between 20.0-31.2 ℃ (see Table A-1).

Mass Balance and Equations

Mass balance calculations provide a means for understanding which fluxes of

methane and the radionuclides are important and which can be discounted within St.

Louis Bay.
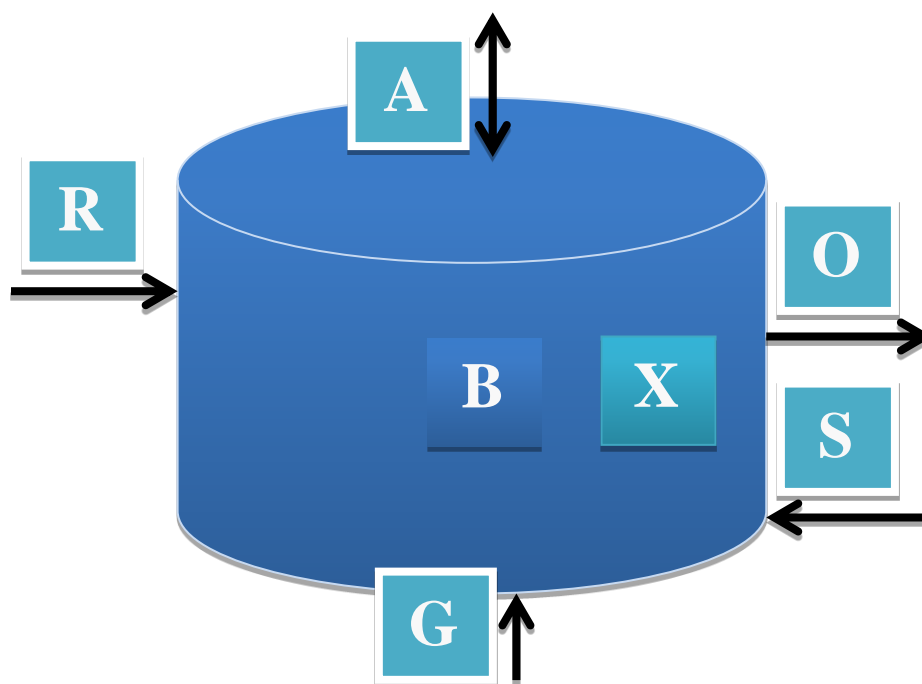
Figure 4. Schematic of St. Louis Bay methane fluxes. R is fluvial flux, A is air-sea equilibration, G is groundwater flux, X is oxidation flux, O is outgoing estuarine water and S is incoming seawater.

Assuming steady state, one can construct five mass balance equations for water,

salt, radon-222, radium-226, and methane. Because the chemical concentrations can

generally be measured, one should be left with five (or fewer) variables and, thus,

uncertain fluxes or processes will be determined. In particular, methane oxidation rates

have been extremely difficult to measure in situ or recreate in the lab. This difficulty is

due to the complex interaction of environmental parameters and the localized nature of

the occurrence of methane oxidation (Borges and Abril, 2011; Abril and Iversen, 2002;

Ding et al., 2003; Kiene, 1991; Topp and Hanson, 1991). As shown below, all fluxes can

be calculated easily with the exception of oxidation. As the last unknown flux, the whole-system methane oxidation rate can be calculated through the use of the mass balance. This technique then completes the hypothesized cycle of methane within St. Louis Bay and can also show the relative importance of each flux in the system.

The methane inventory (B) was calculated by averaging the concentrations found at stations 6, 10, 13, and 14 and multiplying by the volume of the St. Louis Bay. These stations were centrally located within the estuary to best represent the water body as a whole. Additional stations (11, 16, 19) were considered for the interior average concentration of the estuary. However, these stations increased the relative standard deviation of the calculation and did not improve the representation of the interior than calculations without. Therefore, these stations were not used in the final calculation. The highest inventory was observed on 1 August 2013, and the lowest inventory was observed in 29 October 2013 and 30 September 2013. Standard deviations were calculated for the average methane concentration of the interior of the estuary. This standard deviation was divided by the average to get the relative standard deviations presented as percentages in Table 4.

The water balance of the St. Louis Bay contains two sources and one sink. Water enters the estuary through fluvial inputs (R) and incoming seawater (S). Groundwater (G) input of water into the system is assumed negligible in comparison. Water exits the system through outgoing estuarine water (O). Therefore, assuming a steady state, the incoming estuarine water flux (Q_S) in the system can be represented by the following equation:

$$Q_S + Q_R = Q_O$$

River flux was calculated by averaging the entire day's data for the recorded discharge rate from USGS station 02481510 for the Wolf River. This averaged discharge was then multiplied by the concentration of methane from station 4. No discharge data is available for the Jourdan River. Given that the drainage area of the Wolf is 798 sq km and the Jourdan 543 sq km, the discharge rate of the Jourdan was assumed to be 68% of that of the Wolf River (543 sq km/798 sq km). This estimated discharge was then multiplied by the methane concentration from station 4. It should be noted that salinities measured at the river mouth stations were not 0. In a preliminary study, large decreases in methane concentration were observed between the mouths of the rivers and further upstream (see Table A-2, Figure A-2). The actual end-member concentration was therefore unclear. As an estimate of the flux of methane from the *river mouth* (with salinity S_R) into the bay, the river discharge was multiplied by the factor $[1 + S_R/(S_B - S_R)]$, where S_B is the mean salinity of the bay and the second term in the factor gives the ratio of seawater mixed with river water to yield the observed salinity at the river mouth. This scaled discharge is then multiplied by the observed methane concentration at the river mouth to give the flux of methane from the river mouth into the bay. While this calculation is necessarily crude and uncertain, it will be shown below that this is a minor flux of methane into the central part of the bay and, thus, does not matter for the purpose of the mass balance. The relative standard deviation of river discharge was found by dividing the standard deviation of the discharge rate over 24 hours by the average discharge rate over 24 hours.

The salt balance within the estuary has one input and one removal. Salt is added through incoming seawater, and salt is removed via outgoing estuarine water. To find the flux of salt, the following equation is used:

$$S_S \times V_T = S_B(V_T + V_F)$$

Where S_S is the salinity of seawater entering the estuary, V_T is the tidal prism volume, V_F is the river water volume entering the estuary on one tidal cycle, and S_B is the average salinity of the estuary.

Outgoing estuarine water flux was estimated through the tidal prism method (Dyer, 1973). Height of low tide was subtracted from the height of high tide and multiplied by the area of the estuary. The volume of river water flux for that tidal period was added to the tidal prism calculation and represented the final outgoing water flux volume. Salinity from station 20 was used for S_O, and the average salinity of the interior of the estuary was used for S_B.

The mass balance of radium-226 into the system has three inputs and two sinks. Input occurs through the river, incoming seawater, and groundwater flux (F). Groundwater flux is comprised of two components, advective (Q_G) and diffusive (Q_D). Outgoing estuarine water and radioactive decay of radium to radon-222 within the bay (B) are the two sinks. The decay constant of radium is represented by λ_{Ra}. One then gets the following equation:

$$Q_R Ra_R + Q_S Ra_S + F_{G-Ra} = Q_O Ra_O + \lambda_{Ra} Ra_B$$

$$F_{G-Ra} = Q_G Ra_G + Q_D Ra_G$$

The mass balance of radon-222 has four sources and three sinks from the system. Sources include the radioactive decay of radium-226 into radon-222, fluvial input,

incoming seawater, and the groundwater flux. Sinks include outgoing estuarine water,

sea-air exchange (A), and radioactive decay to Po-218.

$$\lambda_{Ra} Ra_B + Q_R Rn_R + Q_S Rn_S + F_{G-Rn} = Q_O Rn_O + F_{A-Rn} + \lambda_{Rn} Rn_B$$

$$F_{G-Rn} = Q_G Rn_G + Q_D Rn_G$$

The methane mass balance of the St. Louis Bay had four major sources into the

estuary and three major sinks. Sources included incoming seawater, groundwater,

sediments, and fluvial input. For the simplification of the box model, sediments and

groundwater flux was considered as a single flux, G. Sinks included the atmosphere,

oxidation, and outflow to the coastal ocean. Ebullition was not measured as previous

studies have shown minimal impacts on water column concentrations (Klein, 2006;

Bastviken et al., 2004; Bugna et al., 1996). Assuming a steady state, the mass balance

was as follows (where K is a first-order rate constant for methane oxidation):

$$Q_R C_R + F_G = Q_O C_O + F_A + K(C_B)$$

Previous studies have shown incoming seawater to be a negligible source of methane,

radon and radium (Burnett and Dulaiova, 2003; Abril and Iversen, 2002; Middleburg et

al., 2002; Scranton and Brewer, 1977; Upstill-Goddard, 2000). Data collected during this

study showed methane concentrations to be very low in the seawater outside of the

estuary (see Figure 3). Additionally, these data have shown residence times of methane

within the estuary to be on the order of hours. Water residence times within the estuary

are markedly longer (see Table 3). Any methane flowing into the estuary from the coastal

ocean would not have an impact on the overall methane balance.

Rearranging the mass balance of radon-22:

$$F_{G-Rn} = Q_O Rn_O + F_{A-Rn} + \lambda_{Rn} Rn_B - \lambda_{Ra} Ra_B - Q_R Rn_R$$

where: $\lambda = 0.181 \ d^{-1}$

$$F_{A-Rn}\frac{dpm}{m^2 hr} = k_w(C_{St\ 6,10,14,15} - \alpha C_{air}) \text{ (Lambert and Burnett, 2003)}$$

α = dimensionless solubility coefficient ~0.2 at 20°C

$$k_w \frac{m}{s} = 0.45\mu^{1.6}\left(\frac{Sc}{600}\right)^{-a} \text{ or } k = 0.91 \text{ if } \mu < 1.5\frac{m}{s}$$

$$\mu = wind\ velocity\frac{m}{s}$$

$$a = 0.667 \text{ if } \mu \leq 3.6\frac{m}{s} \text{ or } 0.5 \text{ if } \mu > 3.6\frac{m}{s}$$

where *Sc* is the Schmidt number with selected values shown below:

$Sc = 1183$ at 15°C (Jähne et al., 1987)

$Sc = 885$ at 20°C (Jähne et al., 1987)

$Sc = 672$ at 25°C (Jähne et al., 1987)

$$F_A(\frac{nmol}{hr}) = k_w(C_{Avg\ St\ 6,10,14,15} - C_o) \times A_{BSL} \text{ (Wanninkof et al., 2009)}$$

C_o = surface film equilibrated with the air

(Wiesenburg and Guinasso, 1979)

$$k_w = 0.27 \times u^2 \times \frac{Sc}{660}^{-0.5} \text{ (Sweeney, 2007)}$$

$$Sc = A + B \times T + C \times T^2 + D \times T^3 + E * T^4 \text{ (Wanninkof et al.,}$$

2009)

A= 2101.20

B= -131.54

C= 4.49

D= -0.09

E= 0.00070663

T= temperature (C)

$$u = U \times \frac{10^{1.4}}{h} \text{ (Large and Pond, 1982)}$$

U =wind speed (m/s)

h =height of wind speed measurement (10 m)

A_{BSL} = Area of Bay St Louis

Oxidation: Found by eliminating the other fluxes in the mass balance

$$K(C_B) = Q_R C_R + F_G - Q_O C_O - F_A$$

Calculations

The methane inventory of St. Louis Bay varied between 2000 moles to 8000 moles (see Table 5) in the interior of the estuary. High relative standard deviations for the inventory were observed for all sampling dates and ranged between 27-134%. Sampling took between 3-4 hours depending on weather. Sampling times, therefore, were longer than methane residence times within the estuary except for October 29 2013. The high relative standard deviations could be due to the time lapse during sampling or due to actual spatial differences in methane concentration. Current data cannot eliminate either possibility

Table 5

Methane inventory in St. Louis Bay, Mississippi.

Date	Methane Inventory (mol)	Average Methane Concentration (mol/m^3)	Methane Inventory Standard Deviation	Methane Inventory RSD
8/1/2013	8000	1.17×10^{-4}	5.2×10^{-5}	44%
9/23/2013	4000	5.83×10^{-5}	4.03×10^{-5}	69%
9/30/2013	2000	3.08×10^{-5}	4.11×10^{-5}	134%
10/8/2013	6000	8.77×10^{-5}	5.82×10^{-5}	66%
10/29/2013	2000	3.40×10^{-5}	9.24×10^{-6}	27%

Environmental conditions varied between sampling dates. The average water temperature within the interior region of the estuary varied between 20.6ºC and 30.4ºC. The relative standard deviation of the temperature measurements of interior stations was below 2% for all samplings (see Table 6). The highest temperature was observed on 1 August 2013, and the lowest was observed on 29 October 2013. The average salinity for the interior of the estuary ranged between 12.0 and 14.5 during the sampling times (see Table 6). The relative standard deviation ranged between 5-16.5%. The highest salinity was observed on 8 October 2013 and the lowest on 1 August 2013. River flux varied considerably between 70 and 400 moles/day (see Table 6), with relative standard deviation of discharge between 9-43%. The greatest river methane flux was observed on 8 October 2013, and the lowest was observed on 29 October 2013. Seawater methane flux varied between 0-900 moles/day leaving the estuary (see Table 6). The highest flux was observed on 8 October 2013 and the lowest flux was observed on 30 September

2013. The highest net rate of oxidation was found to be -40 mol/day, and the lowest

resulted in a gain of methane of 50 mol/day (see Table 6). A positive value indicates a net

addition of methane. Air-sea flux was the largest sink out of the estuary, ranging between

4,000 and 100,000 moles/day (see Table 6). The greatest flux was observed on 1 August

2013, and the lowest flux was observed on 29 October 2013. It should be noted that this

calculation was heavily dependent upon the average methane concentration, which had a

very high relative standard deviation. Methane residence times (i.e., the methane

inventory divided by the air-sea flux) within the St. Louis Bay were calculated to be 2-14

hours, with all residence times of 2 hours except for the 29 October 2013 (see Table 6).

Radon concentrations within St. Louis Bay were low, ranging between .009-.07 Bq/L

(see Table A-3). Radon concentrations were too low for accurate measurements using the

Rad7.

Table 6.

Methane Fluxes in St. Louis Bay, MS

Date	Methane Inventory (mol)	Water Temp (C)	Water Temp RSD	Salinity	Salinity RSD	Oxidation Rate (mol/d)	Fluvial Input (mol/d)	River End Member Calculation (mol/d)	River Discharge RSD	Outgoing Estuarine Water (mol/d)	Air-Sea Flux (mol/d)	Methane Residence Time (hr)
8/1/2013	8000	30.4	0.40%	12	5%	N/A	200	276	23%	90	100000	2
9/23/2013	4000	26	1.60%	14.5	11%	1	400	561	31%	600	50000	2
9/30/2013	2000	26.4	0.60%	13.3	8.10%	1	200	332	43%	0	20000	2
10/8/2013	6000	23.4	1.40%	11.8	16.50%	-40	200	261	9%	900	70000	2
10/29/2013	2000	20.6	0.40%	12.7	7.50%	50	70	97	11%	300	4000	14

Discussion

The discussion is presented in four segments: the effect of air temperature on methane inventory, the oxidation sink, the magnitude of sediment flux, and the magnitude of air-sea equilibration flux.

Methane Inventory and Temperature.

Higher temperatures may result in faster methane production, as most biological processes slow with lower temperature. Soil respiration of CO_2 has been found to slow with lower temperatures, with increasing sensitivity to change with decreasing temperature (Lloyd and Taylor, 1994). Soil temperature and biological processes affecting methane concentration in pore waters were not investigated. However, Schütz et al. (1990) found methane emissions from rice paddy fields to be significantly correlated with daily temperature changes at certain soil depths.

A significant correlation between methane inventory and the average weekly air temperature was not found (see Figure 5). The r^2 value was found to be 0.4, and the p-value was found to be 0.22. However, previous studies have indicated a correlation between air temperature and dissolved methane concentration in wetlands, marshes and rice paddies (Van der Nat and Middleburg, 2000; Nouchi et al., 1994; Schütz et al., 1990; Baker-Blocker et al., 1977). Additionally, a correlation was not observed between water temperature (^{o}C) and inventory.
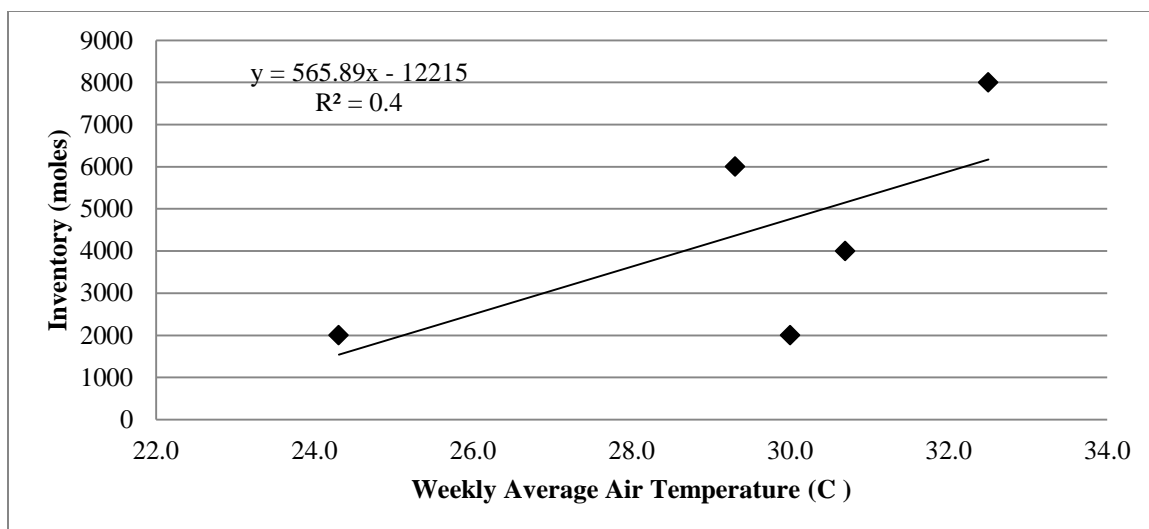
Figure 5. Linear regression of methane inventory in moles (y axis) and average weekly air temperature in celsius (x axis). The r^2 value was found to be 0.4 and the p-value was found to be 0.22. No significant correlation was found.

Oxidation.

Oxidation was hypothesized to be a significant sink of methane within the water column. Utsumi and Norjiri (1998) estimated an average oxidation rate of 12.3 mg CH_4/m^2/day in a shallow, oxic lake (maximum depth 7.3 m). Ignoring differences in water depth, an oxidation rate of this nature would result in a daily loss of 30,000 mol/day of CH_4 (multiplying the flux by the area of the St. Louis Bay) from the St. Louis Bay. de Angelis and Scranton (1993) observed an oxidation rate in the Hudson River and estuary that would have resulted in up to 14,000 mol/day methane oxidation (ignoring differences in depth) within the St. Louis Bay. de Angelis and Scranton (1993) did observe oxidation to dominate over air-sea flux in waters with salinity below 6; however, above this threshold, oxidation was greatly inhibited. Additionally, a 2.1 fold increase was found in oxidation rates with each 10ºC increase in temperature (De Angelis and Scranton, 1993), which is approximately equal to normal microbial increases due to changes in temperature (Atlas and Bartha, 1981).

Methane oxidation is a complex biological process (Borges and Abril, 2011; Murase and Sugimoto, 2005; Abril and Iversen, 2002; Boetius et al., 2000; Utsumi and Nojiri, 1998; de Angelis and Scranton, 1993; Roslev and King, 1995; Kiene, 1991; Alperin and Reeburgh, 1985). Therefore, intensive methane oxidation studies have been conducted to specifically target this flux out of natural water systems. However, this type of work was outside of the scope of this thesis. Therefore, rudimentary incubations were completed (as described in the methods section) but did not find a consistent rate of net oxidation (see Figure 6).

Due to the magnitude of air-sea flux out of the system and the comparably low river flux, a net oxidation rate could not be estimated from the box model. The mass balance could not be closed by the parameters measured. Additionally, salinity was consistently found to be above 6, likely inhibiting methane oxidation (Borges and Abril, 2011; Angelis and Scanton, 1993).The relatively low net oxidation within the experiment and high salinity indicate a negligible oxidation rate for the St. Louis Bay.
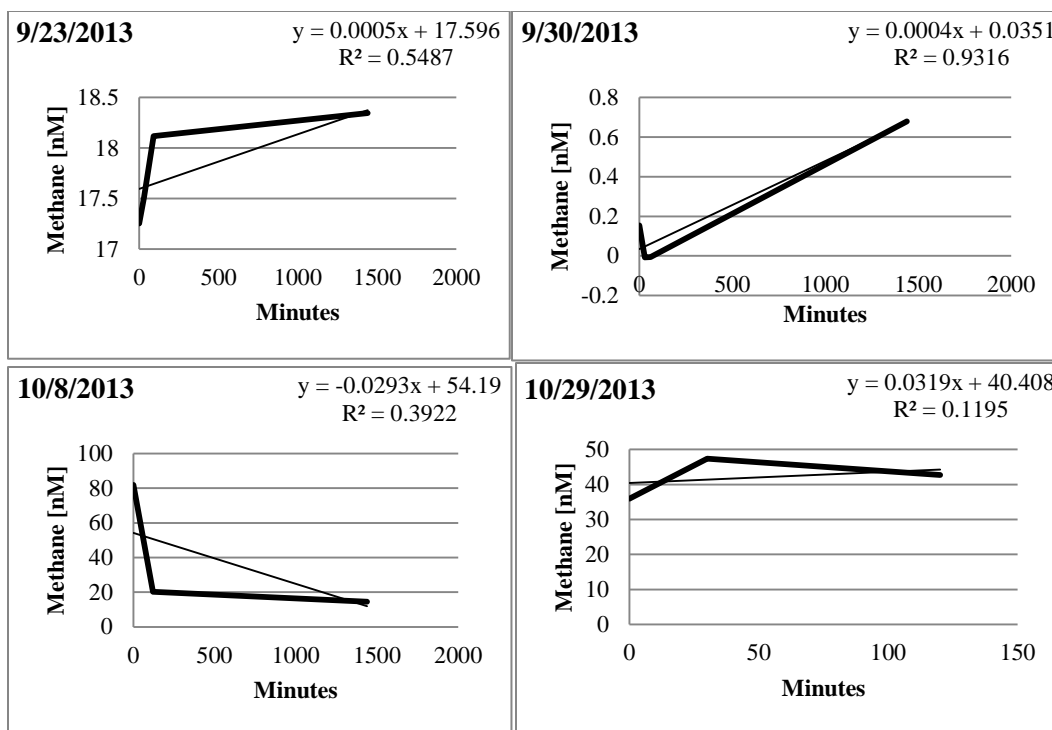
Figure 6. Oxidation incubation experiment results. Oxidation incubations did not yield oxidation rates that were significant in comparison to air-sea flux.

Sediment Flux.

Possible sources of methane to the St. Louis Bay are from river and marsh water discharge and methanogenesis within the system and within submarine groundwater. For the purposes of this study, methanogenesis and submarine groundwater discharge are grouped into sediment flux. As stated in the introduction, sediment flux can be a large source of methane into an estuary (Borges and Abril, 2011; Ding et al., 2003; Abril and Iversen, 2002; Bugna et al., 1996; Marty, 1993; Kiene, 1991; Barnes and Goldberg, 1976). Abril and Iversen (2002) found rates that would equal 120-16,000 mol/day flux out of sediments into the overlying water column within an estuary the size of the St. Louis Bay.

Radon concentrations within the St. Louis Bay proved to be too low for proper measurement with the Rad7 (see Table A-3). An SGD flux could not be calculated using

the data collected. However, low radon concentrations do not eliminate the possibility of SGD flux into the system. The SGD may contain low concentrations of radon or the SGD flux may be too diffuse to measure using this method. It is unlikely that SGD has a point source elsewhere in the estuary. Although interior concentrations of methane varied between stations, there was no single station that consistently showed higher concentrations of methane.

Trace elements are additional indicators of submarine groundwater discharge (Burnett et al., 2006; Shaw et al., 1998; Li and Chan, 1979). Shim (2011) showed trace element additions of a suite of elements within the St. Louis Bay. However, additions of Cs were sourced back to the DuPont factory. The addition of dissolved Ba at mid-salinity indicated desorption or remobilization from reducing sediments. This trace metal data also does not eliminate the possibility of SGD within St. Louis Bay.

The Magnitude of Air-Sea Flux.

The magnitudes of river flux and outgoing estuarine water flux in comparison to the air-sea flux were insignificant with an r^2 of 0.6 and a p-value of 0.13. (see Table 6). If the river concentration was changed to an upstream concentration, fluvial flux would still be negligible in comparison to air-sea flux (see Table 6). The air-sea flux was independent from other fluxes, with methane inventory, wind speed, and methane concentrations in the overlying air dominant factors in its calculation. A significant correlation was not found between air-sea flux and average weekly air temperature (see Figure 7).
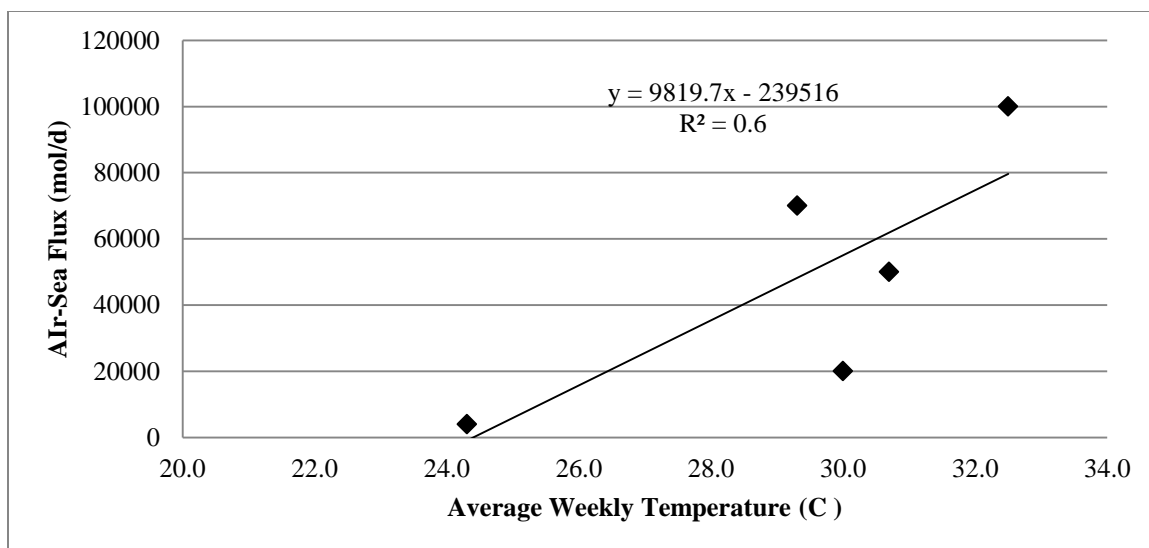
Figure 7. Air-sea flux (mol/d) vs average weekly temperature (C) with r^2 of 0.6 and a p-value of 0.13. No significant correlation was found.

The magnitude of the air-sea flux was compared to previous studies. It was found

that rates of the flux were comparable to other findings from shallow estuaries and

mangroves (see Table 7).

Table 7

Comparison of air-sea flux study findings

Location	St. Louis Bay	Pulicat Lake (Shalini et al., 2006)	Adyar Estuary (Purjava and Ramesh, 2001)	Changning Mangroves (Lu et al., 1999)
Depth (m)	1.3	1-2.5	3-4	N/A
Flux (mol/m^2/d)	2.5×10^{-5} to 2.5×10^{-3}	9.62×10^{-4}	0.03	3.12×10^{-5}
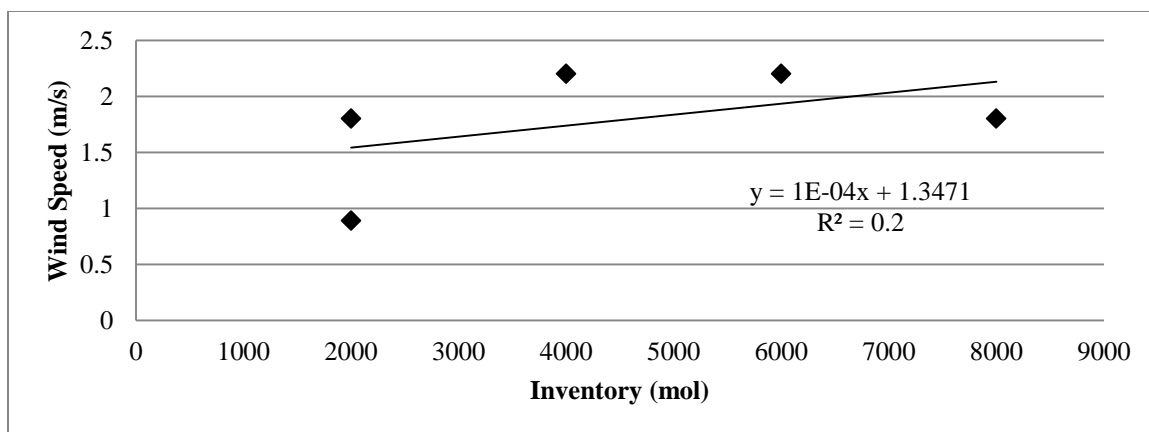
Figure 8. Linear regression of wind speed in m/s (y axis) and methane inventory in moles (x axis). The r^2 was 0.2, and the p-value was 0.42. No significant correlation was found.

No correlation was found between methane inventory and wind speed with an r^2 of 0.2 and a p-value of 0.42. It is noted, however, that very low or very high wind speeds were not observed during the sampling period. Within the St. Louis Bay, wind direction may play a key role in circulation and the magnitude of methane sources. Winds originating in the south have the potential to carry low concentrations of methane into the estuary from the coastal ocean, while winds originating in the north would pull methane rich waters from rivers and marshes. Wind speed was used, however, to calculate the air-sea flux.

If estuaries exhibited similar flux rates to the atmosphere, a global estimation would be 9,000-90,000 mol/year, assuming an approximate area for all estuaries to be 1.5×10^6 km^2 (St. Louis et al., 2000). This estimate would account for <1% to 6% of all natural fluxes of methane to the atmosphere (Kirschke et al., 2013).

Gulf of Mexico.

In the process of developing and testing the methodology of this thesis, open ocean work was completed. Two cruises in the Gulf of Mexico were undertaken in 2011 and 2013. Both included stations at the Deepwater Horizon wellhead and extended into

the surrounding area. The cruise completed in 2013 included the Orca Basin, a mini-basin in the Northern Gulf of Mexico that contains an anoxic brine.

Methane profiles in the Northern Gulf of Mexico rarely deviated from a pattern, (see Figure 9). A slight supersaturation was found at the surface with a maximum near the chlorophyll maximum. A steep decline in concentration occurs with depth to values near to ~1 nM in deeper waters. Not infrequently, a local maximum was observed near the bottom of the profile, indicating possible methane seeps.

Concentrations found in 2010, 2011, and 2013 support the previous study of methane in the northern Gulf of Mexico by Brooks et al. (1981) (see Figures 9 and 10). It should be noted that Brooks et al. (1981) only focused upon the subsurface maximum.

The northern Gulf of Mexico is known for its multitude of methane seeps (Kennicutt et al., 1988a; Kennicutt et al., 1988b; Aharon et al., 1992; Macdonald et al., 1994; Roberts and Carney, 1997; Sassen et al., 1998; Orcutt et al., 2004). It was unknown how these seeps affected concentrations in the overlying water column. The data presented here suggest that methane from seeps in the northern Gulf do not greatly affect background methane concentrations overall. Rather, methane seeps result in small increases in concentration that are quickly brought back to background levels in the surrounding water (see Figures 9 and 10). This loss of methane results in a profile not dissimilar to open ocean work in the Atlantic and Pacific where seeps are not as common (Scranton and Brewer, 1977; Tilbrook and Karl, 1995; Watanabe et al., 1995; Grant et al, 2009).
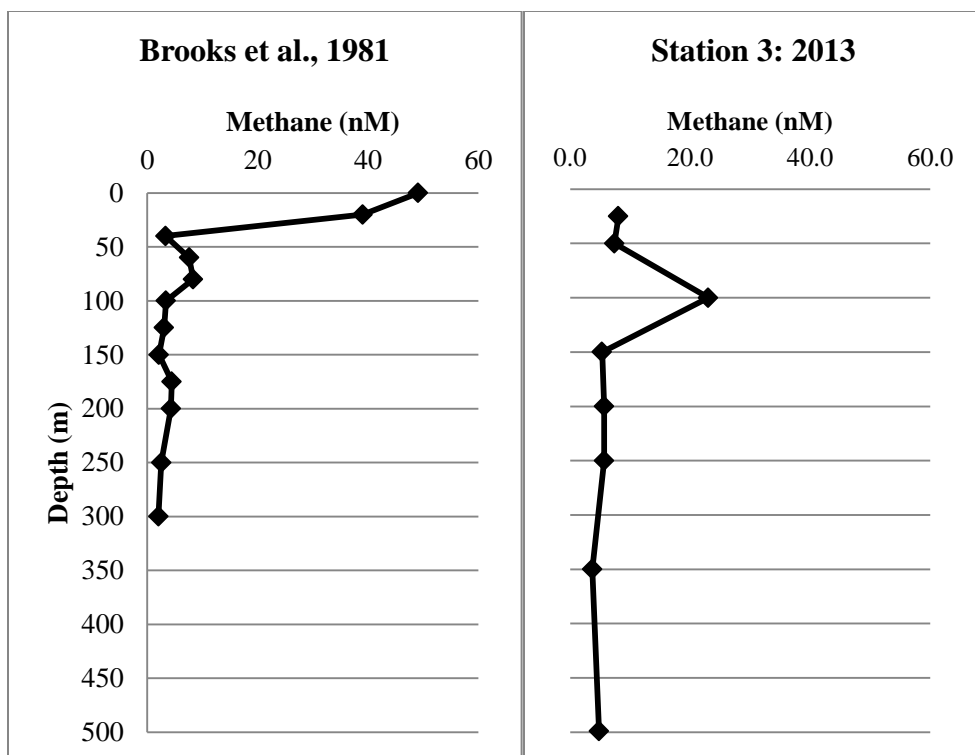
Figure 9. Data from Brooks et al. 1981 and from the 2013 cruise in the Gulf of Mexico. Profiles show comparable concentrations for northern Gulf of Mexico profiles between chromatographic techniques used by Brooks et al. (1981) and CRDS. Profiles collected throughout the northern Gulf of Mexico do not indicate higher concentrations due to methane seeps compared to profiles from the Atlantic and Pacific (Scranton and Brewer, 1977; Tilbrook and Karl, 1995; Watanabe et al., 1995; Grant et al. 2009).

Concentrations measured in the area surrounding the Deepwater Horizon site did not suggest continuing leakage from the wellhead. Profiles from 2010, 2011, and 2013 indicated concentrations indicative of background levels (see Figure 10).
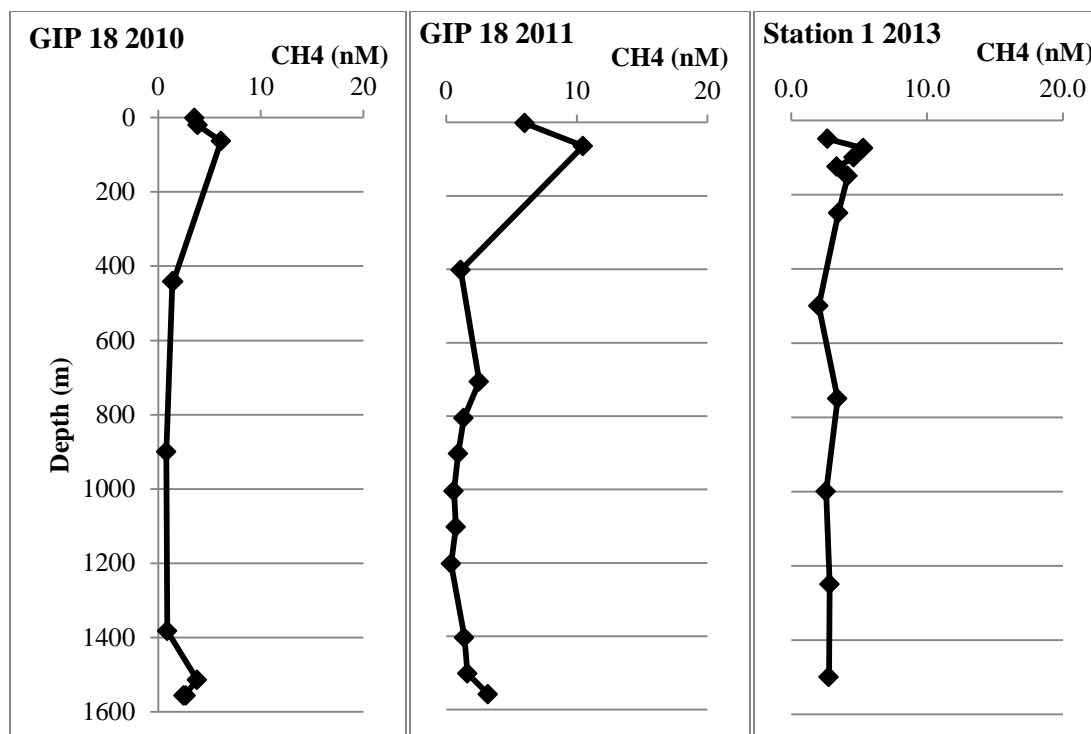
Figure 10. Methane profiles from 2010, 2011 and 2013 at GIP 18 in 2010 and 2011 and station 1 in 2013 in the northern Gulf of Mexico at the Deepwater Horizon Site. Profiles show background level concentrations for all three cruises.

The origin of the maximum observed above 200 m is under debate (Metcalf et al., 2012; Karl et al., 2008; de Angelis and Lee, 1994; Marty, 1993; Sieburth, 1991; Burke et al., 1983; Scranton and Brewer, 1977). The steep decline in methane concentration below the maximum is likely due to oxidation within the water column (Kitidis et al., 2010; Punshon et al., 2014).

The Orca Basin is an intraslope depression located on the Louisiana continental slope (27.011 N, -91.2773 W). Previous research indicated concentrations of approximately 750 μM dissolved CH_4 in the deep hyper-saline waters (with salinity approximately 250 g/L) (Wiesenburg et al., 1985) and a residence time of 5700 years (Sackett et al., 1979). It should be noted that the residence time estimation is problematic due to the limitations in data and invalid assumptions in its calculation that have yet to be

overcome (Sackett et al., 1979; Shah et al., 2013). The high concentrations observed were far outside the range of the Picarro G2301 without great dilution of the sample. Upon retrieval of 60 mL samples into plastic syringes, 60 mL samples of hypersaline water were immediately and tightly enclosed in plastic wrap to minimize leakage of methane out of sample syringe. Zero air was quickly added to each syringe, which was immediately re-wrapped and placed on a shaker table for approximately 30 minutes. Upon equilibration, sample headspaces were diluted to approximately 7% with zero air. Relative standard deviations of these measurements were between 3.4%-10.6%. The equation for Wiesenburg and Guinasso (1979) can be used for any given salinity and temperature.

Dissolved methane concentrations within the water column above the brine were 3.3-8.7 nM (see Figure 11, Table A-4). Concentrations within the brine increased from 2 μM at 1800 m to 630 μM at 2454 m. Measurements just above the brine at 1700 m were 6 nM. These measurements are in agreement with previous concentrations in this basin published by Wiesenburg et al. (1985) and indicate no significant change in the basin's methane inventory over the course of three decades. The sharp gradient suggests minimal mixing with the overlying water column, as would be expected from the extreme salinity gradient.
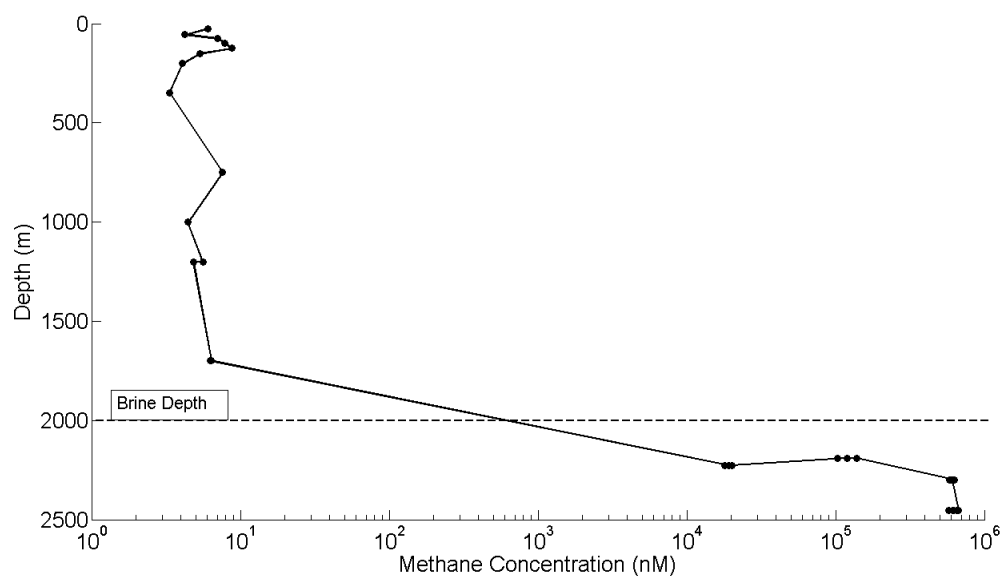
Figure 11. Methane Orca Basin profile collected in October 2013. Brine depth was approximately at 2000m. Low nM concentrations of methane were observed above the brine. Maximum concentrations within the brine reached 630 µM.

CHAPTER V

SUMMARY

Data generated by this study indicates that the major source of methane to St. Louis Bay comes from the sediments, either by diffusion from the porewaters or SGD. The major sink is air-sea equilibration. The data indicate oxidation, river water input, and outgoing estuarine water to be negligible in comparison. Despite the dominance of a single flux and sink, the inventory of St. Louis Bay was complex, depending upon multiple variables. This complexity indicates the fluxes themselves depend upon multiple variables, some of which were not measured in this study. Further work should focus upon the major source and sink of the estuary.

The largest source is inferred to be the sediment flux. The methane residence time is significantly shorter than the water residence times within the estuary (see Table 5). Therefore, river and marsh water discharge cannot account for the resulting methane inventory within St. Louis Bay, nor can they account for the magnitude of the air-sea flux. As the only remaining source, sediment flux therefore accounts for the disparity in the mass balance and is the dominant source of methane into the system. More research is necessary to determine what form of sediment source is important for the methane inventory in the St. Louis Bay. It is possible that SGD waters are not rich in radon or that SGD is too diffuse or simply too low to use radon as an indicator. Additionally, diffusion from porewaters could be partially responsible for the methane inventory.

Additional open ocean work suggests a consistent pattern of methane concentrations within the water column. A slight supersaturation in surface waters, followed by a maximum near the chlorophyll max and a steep decline close to zero are

expected. Data do not suggest that methane seeps affect methane profiles overall. Data also do not suggest continuing leakage from the Deepwater Horizon site, with background levels found in 2010, 2011, and 2013.

The method developed provides accurate and precise methane data in the nM range. High concentrations of methane, such as those found in the Orca Basin brine, can also be measured with alterations to compensate for limitations in the CRDS 2301.

APPENDIX

Table A-1

St. Louis Bay Methane Data. Raw data collected at each station for salinity, temperature and methane concentration.

Date	Station	Salinity	Water Temp (Celsius)	Dissolved Methane (nM)
08-01-2013	1	13.2	30.2	141
	2	11.4	30.0	148
	3	8.3	30.3	124
	4	5.1	30.3	218
	5	11.0	30.8	145
	6	12.1	30.6	40
	7	12.8	31.1	168
	8	12.4	31.2	151
	9	10.2	30.8	120
	10	12.1	30.4	150
	11	10.6	30.8	154
	12	6.0	30.2	151
	13	6.8	30.4	133
	14	11.2	30.3	142
	15	12.5	30.4	137
	16	11.5	30.4	33
	17	10.4	31.0	155
	18	11.4	30.6	6
	19	13.5	30.4	3

Table A-1 (continued).

Date	Station	Salinity	Water Temp (Celsius)	Dissolved Methane (nM)
	20	14.8	30.1	4
09-23-2013	1	16.2	25.7	15
	2	14.3	26.0	39
	3	11.0	26.5	129
	4	8.8	26.8	252
	5	11.5	26.0	235
	6	12.5	25.5	64
	7	12.7	25.1	40
	8	13.2	25.8	155
	9	13.8	25.9	20
	10	14.8	25.8	22
	11	13.6	25.8	26
	12	11.1	26.8	291
	13	14.0	25.9	29
	14	14.8	26.2	17
	15	14.3	26.2	113
	16	16.4	26.4	34
	17	15.9	26.7	177
	18	16.2	26.5	38
	19	14.4	26.4	28
	20	15.9	26.1	37
09-30-2013	1	14.4	26.4	0

Table A-1 (continued).

Date	Station	Salinity	Water Temp (Celsius)	Dissolved Methane (nM)
	2	13.5	26.6	4
	3	10.8	26.0	150
	4	6.7	26.5	166
	5	9.7	26.2	33
	6	12.2	26.2	26
	7	10.9	26.2	4
	8	11.1	26.6	46
	9	12.1	27.1	159
	10	12.8	26.6	0
	11	12.2	27.0	5
	12	11.5	26.9	261
	13	13.3	26.8	166
	14	13.6	26.4	90
	15	14.7	26.4	6
	16	16.6	26.8	4
	17	16.0	27.0	188
	18	16.8	26.9	0
	19	16.8	26.9	0
	20	17.9	26.8	0
10-08-2013	1	12.6	22.9	53

Table A-1 (continued).

Date	Station	Salinity	Water Temp (Celsius)	Dissolved Methane (nM)
10-08-2013	1	12.6	22.9	53
	2	10.3	23.7	69
	3	9.3	24.3	104
	4	7.8	25.0	256
	5	8.9	23.2	115
	6	9.4	23.0	96
	7	11.0	23.3	43
	8	11.8	22.1	599
	9	13.0	23.4	15
	10	12.6	23.3	15
	11	13.3	22.8	40
	12	6.0	24.1	283
	13	13.0	23.0	51
	14	13.9	23.4	82
	15	11.1	23.8	157
	16	14.3	23.5	105
	17	15.1	24.3	426
	18	13.8	23.4	90
	19	13.0	23.6	65
	20	14.6	23.8	40

Table A-1 (continued).

Date	Station	Salinity	Water Temp (Celsius)	Dissolved Methane (nM)
10-29-2013	1	12.9	20.5	36
	2	12.7	20.0	33
	3	10.6	20.0	69
	4	9.0	20.6	303
	5	10.3	20.8	61
	6	11.7	20.6	35
	7	10.6	20.7	63
	8	10.9	20.7	104
	9	11.9	21.2	44
	10	12.2	20.5	22
	11	12.3	21.1	65
	12	10.6	20.9	45
	13	12.8	20.6	355
	14	12.8	20.7	36
	15	13.9	20.6	44
	16	14.6	20.8	47
	17	14.3	21.2	90
	18	15.4	20.8	28
	19	15.3	20.6	25
	20	15.6	20.8	25

Table A-2

Preliminary St. Louis Bay Methane Data. Displaying maximum methane concentrations at river mouths.

Date	Station	Latitude Decimal Degrees	Longitude Decimal Degrees	Salinity	Water T	nM CH4
07-17-13	1	30.334135	-89.330784	1.1	28	20
	2	30.342385	-89.33839	8.1	27	58
	3	30.340334	-89.354371	4.8	28	54
	4	30.335621	-89.371846	3.4	28	60
	5	30.341397	-89.400549	2.2	28	107
	6	30.365013	-89.40039	1.2	28	392
	7	30.346904	-89.37318	5.8	28	80
	8	30.35207	-89.365104	6.1	28	73
	9	30.361638	-89.358667	6.4	28	85
	10	30.372323	-89.341736	8.9	29	77
	11	30.375006	-89.322577	8.6	29	117
	12	30.373291	-89.309933	9.0	29	86
	13	30.367738	-89.310374	8.6	29	81
	14	30.360521	-89.312522	7.9	29	107
	15	30.364727	-89.300306	6.9	29	204
	16	30.358846	-89.289972	8.2	29	220
	17	30.36935	-89.26135	2.0	28	524
	18	30.365392	-89.258818	1.3	28	357

Table A-2 (continued).

Date	Station	Latitude Decimal Degrees	Longitude Decimal Degrees	Salinity	Water T	nM CH4
	19	30.351385	-89.284377	14.7	29	121
	20	30.342446	-89.273393	14.1	29	96
	21	30.341979	-89.256623	14.6	29	61
	22	30.334703	-89.279293	17.1	30	67

Figure A-1. Sampling Station Locations for 17 July 2013.
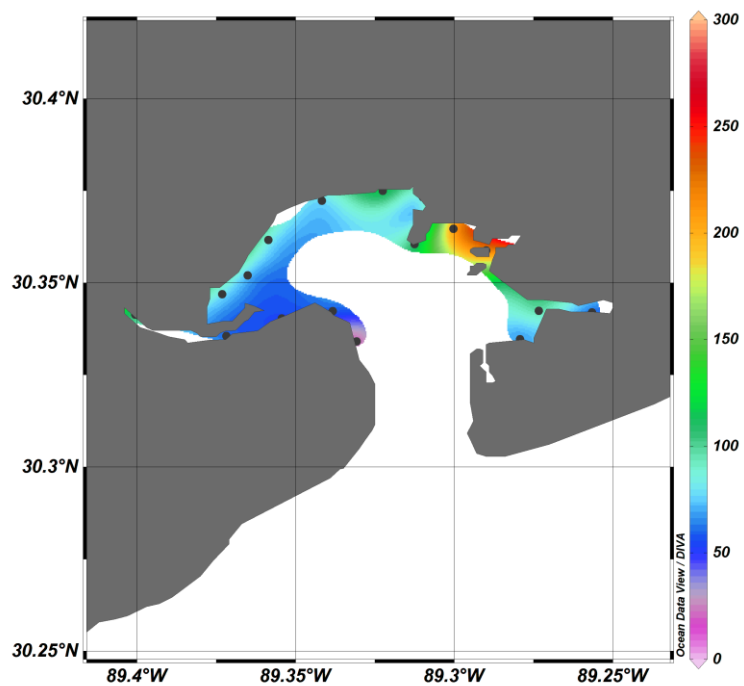
Figure A-2. Sampling for 17 July 2013. Sampling Results using Ocean Data View DIVA Gridding of nM CH₄ concentrations.

Table A-3

Radon St. Louis Bay Data Collected at Station 14.

Date	Bottle	Radon (Bq/L)	Capture SD	Average	SD	RSD	Radium (Bq/L)	Capture SD	Average	SD	RSD	Radon from SGD (Bq/L)
8/1/2013	1	0.0787	0.019				0.0363	0.012				
	2	0.05	0.019				0.034	0.012				
	3	0.0605	0.017	0.063	0.015	23%	0.0454	0.013	0.039	0.006	16%	
	Background	0.0112	0.006				0	0.003				0.01
9/23/2013	1	0.0302	0.015				0.0148	0.008				
	2	0.0184	0.01				0.0114	0.007				
	3	0.0191	0.01	0.0145	0.007	29%	0.0158	0.007	0.014	0.002	16%	
	Background	0.009	0.008				0.007	0.05				0.01
9/30/2013	1	0.0309	0.014				0.00942	0.13				
	2	0.0171	0.011	0.024	0.01	41%	0.0163	0.18	0.015	0.005	35%	
	Background	0	0.045				0.0197	0.009				0.009
10/8/2013	1	0.0179	0.01				0.0158	0.007				
	2	0.0165	0.008				0.0114	0.007				
	3	0.0237	0.009	0.019	0.004	20%			0.014	0.003	23%	
	Background	0.011	0.008				0.014	0.5				0.009
10/29/2013	1	0.0666	0.019				0.0183	0.008				
	2	0.0342	0.013				0.0127	0.008				
				0.05	0.023	45%			0.0137	0.004	31%	
	Background	0	0.01				0.032	0.008				0.07

Table A-4

Gulf of Mexico Field Work 2011Cruise

Station	Latitude Degrees Decimal Minutes	Longitude Degrees Decimal Minutes	Depth	nM CH4
GIP4	28 57.25 N	088 56.09 W	130	13
			130	13
			73	7
			73	8
			5	34
			5	34
GIP6	28 30.69 N	089 48.49 W	4	11
			4	11
			29	11
			29	12
			104	3
			104	3
			504	5
			504	5
			524	5
			524	6
GIP7	28 14.35 N	089 07.33 W	1129	5
			1004	2
			503	2
			105	8
			55	10
			29	4
			8	4
			3	4
GIPK	28 23.19 N	088 52.04 W	3	4
			29	7
			59	10
			105	8
			405	0
			1004	1
			1337	13
GIP11	28 14.02 N	088 21.64 W	3	3
			29	4

Table A-4 (continued).

Station	Latitude Degrees Decimal Minutes	Longitude Degrees Decimal Minutes	Depth	nM CH4
			49	12
			104	6
			506	0
			1004	0
			1104	0
			1968	2
GIPI	28 32.64 N	088 28.12 W	2	5
			28	3
			63	12
			106	6
			505	0
			1005	0
			1204	1
			1503	1
			1738	3
GIPH	28 35.12 N	088 30.70 W	2	4
			29	4
			65	17
			105	6
			505	1
			1004	1
			1104	1
			1405	0
			1503	3
			1702	2
GIP17	28 38.34 N	088 31.08 W	2	5
			30	4
			70	10
			70	10
			105	7
			505	1
			1004	0
			1504	3
			1581	3
			1581	3

Table A-4 (continued).

Station	Latitude Degrees Decimal Minutes	Longitude Degrees Decimal Minutes	Depth	nM CH4
GIP13	28 40.08 N	088 52.32 W	2	5
			29	9
			70	11
			104	6
			503	2
			704	4
			1022	2
GIPM	28 41.43 N	088 44.13 W	2	4
			27	4
			49	10
			105	7
			144	7
			402	1
			503	1
			604	1
			703	2
			804	1
			905	1
			1003	2
			1212	5
GIPG	28 41.11 N	088 33.16 W	2	4
			29	5
			59	9
			103	7
			504	1
			705	1
			1004	2
			1104	1
			1205	1
			1303	1
			1399	3
GIP15	28 44.33 N	088 33.66 W	2	6
			28	11
			64	5
			107	9

Table A-4 (continued).

Station	Latitude Degrees Decimal Minutes	Longitude Degrees Decimal Minutes	Depth	nM CH4
			403	1
			504	1
			703	1
			903	1
			1004	1
			1103	2
			1182	2
GIPB	28 44.58 N	088 28.88 W	11	6
			28	5
			60	11
			104	10
			503	3
			703	1
			1104	2
			1203	2
			1304	1
			1413	1
GIPA	28 48.87 N	088 26.40 W	2	4
			29	4
			51	14
			105	8
			404	1
			505	2
			705	0
			904	1
			904	1
			1005	1
			1104	2
			1241	1
GIPC	28 46.13 N	088 25.89 W	2	5
			66	12
			404	1
			703	2
			803	2
			903	1

Table A-4 (continued).

Station	Latitude Degrees Decimal Minutes	Longitude Degrees Decimal Minutes	Depth	nM CH4
			1004	1
			1104	2
			1204	1
			1303	1
			1382	1
GIP24	28 46.25 N	088 22.85 W	2	6
			58	10
			404	1
			704	1
			804	0
			904	1
			1004	1
			1104	2
			1204	1
			1304	1
			1404	2
GIP18	28 44.33 N	088 20.37 W	2	6
			65	10
			402	1
			706	3
			806	1
			903	1
			1004	1
			1102	1
			1203	0
			1404	1
			1501	2
			1558	3
GIP16	28 43.79 N	088 24.60 W	2	5
			63	12
			404	1
			704	1
			804	2
			904	2
			1004	1

Table A-4 (continued).

Station	Latitude Degrees Decimal Minutes	Longitude Degrees Decimal Minutes	Depth	nM CH4
			1104	1
			1203	1
			1304	1
			1403	1
			1506	4
			1530	3
GIPD	28 41.38 N	088 22.59 W	2	5
			63	21
			404	1
			804	1
			902	1
			1004	1
			1104	1
			1204	1
			1303	0
			1504	3
			1605	1
			1622	1
GIPE	28 38.34 N	088 21.04 W	2	9
			63	10
			63	9
			404	1
			804	0
			904	1
			1004	1
			1203	0
			1303	0
			1494	1
			1604	1
			1712	1
GIPJ	28 35.65 N	088 18.97 W	2	8
			58	10
			405	2
			803	1
			1004	2

67

Table A-4 (continued).

Station	Latitude Degrees Decimal Minutes	Longitude Degrees Decimal Minutes	Depth	nM CH4
			1205	1
			1404	1
			1604	1
			1804	7
			1851	7
GIP25	28 55.49 N	088 19.56 W	2	5
			76	12
			149	4
			405	1
			804	0
			904	0
			1005	0
			1104	2
			1156	1
GIP23	28 51.69 N	088 11.77 W	1	4
			65	10
			65	10
			405	1
			805	0
			905	0
			1005	1
			1106	1
			1205	0
			1304	1
			1350	0
GIP20	28 45.38 N	088 09.60 W	2	6
			62	17
			405	1
			804	0
			1004	0
			1205	0
			1403	0
			1604	0
			1756	1
GIPF	28 42.65 N	088 14.45 W	2	6

Table A-4 Continued

Station	Latitude Degrees Decimal Minutes	Longitude Degrees Decimal Minutes	Depth	nM CH4
			62	12
			405	1
			804	0
			1003	0
			1204	0
			1402	1
			1603	0
			1733	1

Table A-5

Gulf of Mexico Field Work 2013 Cruise.

Station	Latitude Decimal Degrees	Longitude Decimal Degrees	Depth (m)	Salinity	CH4 (nM)
1	28.6355	-88.5156	50	36.6	3
			75	36.6	5
			100	36.6	5
			125	36.4	3
			150	36.2	4
			250	35.6	4
			500	35	2
			750	34.9	3
			1000	34.9	3
			1250	35	3
			1500	35	3
2	28.3231	-89.044	25	36.3	14
			50	36.4	8
			75	36.5	9
			100	37	19
			125	36.4	7
			150	36.3	5
			200	36	9
			250	35.7	3
			350	35.3	3
			500	35	5
			750	34.9	3

Table A-5 (continued).

Station	Latitude Decimal Degrees	Longitude Decimal Degrees	Depth (m)	Salinity	CH4 (nM)
			900	34.9	4
3	27.7118	-89.929	25	36.3	8
			50	36.5	7
			100	36.5	23
			150	36.5	5
			200	36.1	6
			250	35.9	6
			350	35.4	4
			499	35.1	5
			750	34.9	6
			984	34.9	13
4	27.5712	-90.8669	25	35	3
			75	35	4
			100	35	7
			125	35	7
			150	35	4
			200	35	3
			250	35	4
			350	35	4
			500	35	2
			750	35	2
			1150	35	4
5	27.2737	-91.1305	150	35	2
			500	35	1
			1100	35	2
			1400	35	3
			1400	35	3
			1700	35	2
			1700	35	2
			1750	35	1
			1750	35	1
6 (Cast 1)	27.011	-91.2773	25	35	6
			55	35	4
			75	35	7
			100	35	8
			125	35	9
			150	35	5
			200	35	4

Table A-5 Continued

Station	Latitude Decimal Degrees	Longitude Decimal Degrees	Depth (m)	Salinity	CH4 (nM)
			350	35	3
			750	35	8
			1000	35	4
			1200	35	6
			1200	35	5
			1700	35	6
			1700	35	6
			2227	90	19046
			2227	90	17928
			2227	90	20084
(Cast 2)			1800	35	2335
			2000	35	3816
			2000	35	3413
			2190	90	119385
			2190	90	102788
			2000	35	3413
			2190	90	119385
			2190	90	102788
			2190	90	138742
			2300	250	630728
			2300	250	584148
			2300	250	591757
			2300	250	609546
			2454	250	671757
			2454	250	574442
			2454	250	613861
			2454	250	653588
			2454	250	621560
			2454	250	649584

REFERENCES

Abril, G., N Iversen. 2002. Methane dynamics in a shallow non-tidal estuary (Randers Fjord, Denmark). Mar. Ecol.: Prog. Ser. 230: 171-181.

Aharon, P., H. Roberts, R. Snelling. 1992. Submarine venting of brines in the deep Gulf of Mexico: Observations and geochemistry. Geology 20:483-486.

Albert D., C. Martens, M. Alperin. 1998. Biogeochemical processes controlling methane in gassy coastal sediments- Part 2: groundwater flow control of acoustic turbidity in Eckernförde Bay Sediments. Cont. Shelf Res. 18: 1771-1793.

Alexander, A. 2006. Flowing Liquid-Sheet Jet for Cavity Ring-Down Absorption Measurements. Anal. Chem. 78:5597-5600.

Alperin, M., W. Reeburgh. 1985. Inhibition experiments on anaerobic methane oxidation. Appl. Eviron. Microbiol. 50: 940-945.

Atlas, R., R. Bartha. 1981. Microbial Ecology: Fundamentals and Applications. Addison-Wesley Pub. Co.

Baker-Blocker, A., T. Donahue, K. Mancy. 1977. Methane flux from wetland areas. Tellus, Ser. B. 29: 245-250.

Bange, H. 2006. Nitrous oxide and methane in European coastal waters. Estuarine, Costal Shelf Sci. 70: 361-374.

Barnes, R., E. Goldberg. 1976. Methane production and consumption in anoxic marine sediments. Geology. 4: 297-300.

Bartlett, K., D. Bartlett, R. Harriss, D. Sebacher. 1987. Methane emissions along a salt marsh salinity gradient. Biogeochemistry. 4: 183-202.

Bastviken, D., L. Tranvik, J. Downing, P. Crill, A. Enrich-Prast. 2011. Freshwater
Methane Emissions Offset the Continental Carbon Sink. Science. 7:50.

Bastviken, D., J. Cole, M. Pace, L. Tranvik. 2004. Methane emissions from lakes:
Dependence of lake characteristics, two regional assessments, and a global
estimate. Global Biogeochem. Cycles. 18.

Battino, R., H. Clever. 1966. The solubility of gases in liquids. Chem. Rev. 66.4:395-463.

Becker, M., N. Andersen, B. Fiedler, P. Fietzek, A. Körtzinger, T. Steinhoff and G.
Friedrichs. 2012. Using cavity ringdown spectroscopy for continuous monitoring
of $\delta^{13}C(CO_2)$ and fCO_2 in the surface ocean. Limnol. Oceanogr.: Methods. 10:
752-766.

Bera, G. 2014. . Ph.D. thesis. Univ. of Southern Mississippi.

Boetius, A., K. Ravenschalg, C. Schubert, D. Rickert, R. Widdel, A. Gieseke, R. Amann,
B. Jørgensen, U. Witte, O. Pfannkuche. 2000. A marine microbial consortium
apparently mediating anaerobic oxidation of methane. Nature. 407: 623-626.

Borges, A., G. Abril. 2011. Carbon Dioxide and Methane Dynamics in Estuaries In:
Wolanski E and McLusky DS (eds.) Treatise on Estuarine and Coastal Science. 5:
119-161. Waltham: Academic Press.

Brooks, J., M. David, D. Reid, B. Bernard. 1981. Methane in the upper water column of
the northwestern Gulf of Mexico. J. Geophys. Res.: Oceans. 86:11029-11040.

Bugna, G., J. Chanton, J. Cable, W. Burnett, P. Cable. 1996. The importance of
groundwater discharge to the methane budgets of nearshore and continental shelf
waters of the northeastern Gulf of Mexico. Geochim. Cosmochim. Acta. 60:
4735-4746.

Burke, R., D. Reid, J. Brooks, D. Lavoie. 1983. Upper water column methane
    geochemistry in the eastern tropical North Pacific. Limnol. Oceanogr. 28: 10-32.

Burnett, W., P. Aggarwal, A. Aureli, H. Bokuniewicz, J. Cable, M. Charette, E. Kontar,
    S. Krupa, K. Kulkarni, A. Loveless, W. Moore, J. Oberdorfer, J. Oliveira, N.
    Ozyurt, P. Povinec, A. Privitera, R. Rajar, T. Ramessur, J. Scholten, T. Stieglitz,
    M. Taniguchi, J. Turner. 2006. Quantifying submarine groundwater discharge in
    the coastal zone via multiple methods. Sci Total Environ. 367:498-543.

Burnett, W., H. Dulaiova. 2003. Estimating the dynamics of groundwater input into the
    coastal zone via continuous radon-222 measurements. J. Environ. Radioact. 69:
    21-35.

Burnett, W., M. Taniguchi, J. Oberdorfer. 2001. Measurement and significance of the
    direct discharge of groundwater into the coastal zone. J. Sea Res. 46: 109-116.

Busch, K.W. and M.A. Busch. (1999). "Cavity ring-down spectroscopy: An ultratrace
    absorption measurement technique." ACS Symp. Ser. 720, Oxford.

Cable, J., W. Burnett, J. Chanton, G. Weatherly. 1996. Estimating groundwater discharge
    into the northeastern Gulf of Mexico using radon-222. Earth Planet. Sci. Lett.
    144: 591-604.

Cicerone, R., R. Oremland. 1988. Biogeochemical Aspects of Atmospheric Methane.
    Global Biogeochem. Cycles 2: 299-327.

Cook, W., D. Hanson. 1957. Accurate measurement of gas solubility. Rev. Sci. Instrum.
    28: 370-374.

Corbett, R., J. Chanton, W. Burnett, K. Dillon, C. Rutkowski. 1999. Patterns of
    groundwater discharge into Florida Bay. Limnol. Oceanogr. 44:1045-1055.

Crosson, E. 2008. A cavity ring-down analyzer for measuring atmospheric levels of methane, carbon dioxide, and water vapor. Appl. Phys. B: Lasers Opt. 92: 403-408.

de Angelis, M., C. Lee. 1994. Methane production during zooplankton grazing on marine phytoplankton. Limnol. Oceanogr. 39: 1298-1308.

de Angelis, M. and M. Scranton. 1993. Fate of methane in the Hudson River and Estuary. Global Biogeochem. Cycles 7:509-523.

Ding, W., Z. Cai, H. Tsuruta, X. Li. 2003. Key factors affecting spatial variation of methane emissions from freshwater marshes. Chemosphere. 51: 167-173.

Dyer, K. 1973. Estuaries: A Physical Introduction, 1st edition. John Wiley and Sons, London, England.

Eleuterius, C. 1984. Application of a hydrodynamic numerical model to the tides of St. Louis Bay, Mississippi. Journal of the Mississippi Academy of Sciences. 29: 37-48.

EPA. 2010. Methane and Nitrous Oxide Emissions from Natural Sources. U.S. Environmental Protection Agency, Washington, DC, USA.

Etheridge, D., G. Pearman, P. Fraser. 1992. Changes in tropospheric methane between 1841 and 1978 from a high accumulation-rate Antarctic ice core. Tellus B 44: 282-294.

Fung, I., J. John, J. Lerner, E. Matthews, M. Prather, L. Steele, P. Fraser. 1991. Three-dimensional model synthesis of the global methane cycle. Journal of Geophys. Res.: Atmos. 96:13033-13065.

Grant, F., R. Upstill-Goddard, N. Gist, C. Robinson, G. Uher, E. Malcolm, S. Woodward. 2009. Nitrous oxide and methane in the Atlantic Ocean between 50°N and 52°S: Latitudinal distribution and sea-to-air flux. Deep Sea Res. II 56:964-976.

Hallock, A., E. Berman and R. Zare. 2002. Direct Monitoring of Absorption in Solution by Cavity Ring-Down Spectroscopy. Anal. Chem. 74: 1741-1743.

Hussain, N., T. Church, G. Kim.1999. Use of 222-Rn and 226-Ra to trace groundwater discharge into the Chesapeake Bay. Mar. Chem. 65: 127-134.

Ioffe, B., A. Vitenberg. 1984. Head-space analysis and related methods in gas chromatography. New York: Wiley.

Jähne, B., G. Heinz, W. Dietrich. 1987. Measurement of the diffusion coefficients of sparingly soluble gases in water. Journal of Geophys. Res. 92: 10767-10776.

Johannes, R. 1980. Ecological Significance of the submarine discharge of groundwater. Mar. Ecol. Prog. Ser. 3: 365-373

Karl, D., L. Beversdorf, K. Björkman, M. Church, A. Martinez, E. Delong. 2008. Aerobic production of methane in the sea. Nature Geoscience. 1: 473-478.

Kennicutt, M., J. Brooks, G. Denoux. 1988a. Leakage of deep, reservoired petroleum to the near surface on the Gulf of Mexico Continental slope. Mar. Chem. 24:39-59.

Kennicutt, M., J. Brooks, R. Bidigare, G. Denoux. 1988b. Gulf of Mexico hydrocarbon seep communities- 1. Regional distribution of hydrocarbon seepage and associated fauna. Deep Sea Res. Part A. Oceanogr. Res. Papers 35: 1639-1651.

Kiene, R. 1991. Production and consumption of methane in aquatic systems. Microbial production and consumption of greenhouse gases: Methane, nitrogen oxides and halomethanes. American Society for Microbiology. 111-146.

Kiene R., D. Capone. 1988. Microbial transformations of methylated sulfur compounds in anoxic salt marsh sediments. Microb. Ecol. 15: 275-291.

Kim, G., D.W. Hwang. 2002. Tidal pumping of groundwater into the coastal ocean revealed from submarine 222-Rn and CH_4 monitoring. Geophys. Res. Lett. 29: 23-1.

Kipphut, G., C. Martens. 1982. Biogeochemical cycling in an organic-rich coastal marine basin- 3. Dissolved gas transport in methane-saturated sediments. Geochim. et Cosmochim. Acta 46: 2049-2060.

Kirschke, S., P Bousquet, P. Ciais, M. Saunois, J. Canadell, E. Dlugokencky, P. Bergamaschi, D. Bergmann, D. Blake, L. Bruhwiler, P. Cameron-Smith, S. Castaldi, F. Chevallier, L. Feng, A. Fraser, M. Heimann, E. Hodson, S. Houweling, B. Josse, P. Fraser, P. Krummel, J.F. Lamarque, R. Langenfelds, C. Le Quéré, V. Naik, S. O'Doherty, P. Palmer, I. Pison, D. Plummer, B. Poulter, R. Prinn, M. Rigby, B. Ringeval, M. Santini, M. Schmidt, D. Shindell, I. Simpson, R. Spahni, L. 2013. Three decades of global methane sources and sinks. Nature Geoscience. 6: 813-823

Kitidis, V., R. Upstill-Goddard, L. Anderson. 2010. Methane and nitrous oxide in surface water along the North-West Passage, Arctic Ocean. Mar. Chem. 121: 80-86.

Klein, S. 2006. Sediment porewater exchange and solute release during ebullition. Mar. Chem. 102: 60-71.

Kolb, B., L. Ettre. 2006. Static Headspace-Gas Chromatography: Theory and Practice. John Wiley & Sons.

Lambert, M., W. Burnett. 2003. Submarine groundwater discharge estimates at a Florida

    coastal site based on continuous radon measurements. Biogeochemistry 66: 55-

    73.

Large, W. and S. Pond. 1982. Sensible and Latent Heat Flux Measurements over the

    Ocean. J. Phy. Oceanogr. 12:464-482.

Lee, J., and G. Kim. 2006. A simple and rapid method for analyzing radon in coastal and

    ground waters using radon-in-air monitor. J. Environ. Radioact. 89:219-228.

Li, Y., L. Chan. 1979. Desorption of Ba and ^{226}Ra from river-borne sediments in the

    Hudson estuary. Earth Planet. Sci. Lett. 43: 343-350.

Lloyd, J., J. Taylor. 1994. On the Temperature Dependence of Soil Respiration.

    Functional Ecology. 8: 315-323.

Lu, C., Y. Wong, N. Tam, Y. Ye, P. Lin. 1999. Methane flux and production from

    sediments of a mangrove wetland on Hainan Island, China. Mangroves and Salt

    Marshes. 3: 41-49.

Macdonald, I., N. Guinasso, R. Sassen, J. Brooks, L. Lee, K. Scott. 1994. Gas hydrate

    that breaches the sea floor on the continental slope of the Gulf of Mexico.

    Geology 22:699-702.

Martens, C., J. Klump. 1984. Biogeochemical cycling in an organic-rich coastal marine

    basin 4. An organic carbon budget for sediments dominated by sulfate reduction

    and methanogenesis. Geochim. Cosmochim. Acta 48: 1987-2004.

Martens, C., R. Berner. 1977. Interstitial water chemistry of anoxic Long Island Sound

    sediments. 1. Dissolved gases. Limn. Oceanogr.. 22: 10-25.

Marty, D. 1993. Methanogenic bacteria in seawater. Limnol. Oceanogr. 38: 452-456

Matthews, E., I. Fung. 1987. Methane emission from natural wetlands: Global

distribution, area, and environmental characteristics of sources. Global

Biogeochem. Cycles 1:61-86.

McAuliffe, C. 1963. Solubility in water of C_1-C_9 hydrocarbons. Nature. 200: 1092-1093.

Metcalf, W., B. Griffin, R. Cicchillo, J. Gao, S. Janga, H. Cooke, B. Circello, B. Evans,

W Martens-Habbena, D. Stahl, W. van der Donk. 2012. Synthesis of

Methylphosphonic Acid by Marine Microbes: A source for Methane in the

Aerobic Ocean. Science. 337: 1104-1107.

Middleburg, J., J. Nieuwenhuize, N. Iversen, N. Høgh, N. De Wilde, W. Helder, R.

Seifert, O. Christof. 2002. Methane distribution in European tidal estuaries.

Biogeochemistry. 59: 95-119.

Murase, J., Sugimoto. 2005. Inhibitory effect of light on methane oxidation in the pelagic

water column of a mesotrophic lake (Lake Biwa, Japan). Limnol. Oceanogr. 50:

1339-1343.

Nouchi, I., T. Hosono, K. Aoki, K. Minami. 1994. Seasonal variation in methane flux

from rice paddies associated with methane concentration in soil water, rice

biomass and temperature, and its modeling. Plant Soil Sci. 161:195-208.

Orcutt, B., A. Boetius, S. Lugo, I. MacDonald, V. Samarkin, S. Joye. 2004. Life at the

edge of methane ice: microbial cycling of carbon and sulfur in Gulf of Mexico gas

hydrates. Chem. Geology 205:239-251.

Pearson, T., R. Rosenberg. 1978. Macrobenthic succession in relation to organic

enrichment and pollution of the marine environment. Oceanogr. Mar. Biol. Ann.

Rev. 16: 229-311.

Phelps, E. 1999. Environmental quality of Saint Louis Bay, Mississippi. M.S. thesis. The University of Southern Mississippi.

Picarro. 2008. A cavity ring-down analyzer for measuring atmospheric levels of methane, carbon dioxide, and water vapor. Appl. Phys. B 92: 403-408.

Punshen, S., K. Axetsu-Scott, C. Lee. 2014. On the distribution of dissolved methane in Davis Strait, North Atlantic Ocean. Mar. Chem. 161:20-25.

Purjava R., R. Ramesh. 2001. Natural and anthropogenic methane emission from coastal wetlands of South India. Environ. Manage. 27:547-557.

Reeburgh, W. 2007. Oceanic Methane Biogeochemistry. Chem Rev. 107:486-513.

Reeburgh, W., B. Ward, S. Whalen, K. Sandbeck, K. Kilpatrickt, L, Kerkhof. 1991. Black Sea methane geochemistry. Deep-Sea Res., Part A 38:S1189-S1210.

Roberts, H., R. Carney. 1997. Evidence of episodic fluid, gas and sediment venting on the northern Gulf of Mexico continental slope. Econ. Geol. 92:863-879.

Roslev, P., G. King. 1995. Aerobic and anaerobic starvation metabolism in methanotrophic bacteria. Appl. and Environ. Microbiol. 61: 1563-1570.

Sackett, W., J. Brooks, B. Bernard, C. Schwab, H. Chung, R. Parker. 1979. A carbon inventory for Orca Basin brines and sediments. Earth and Planet. Sci. Lett. 44:73-81.

Santos, I., N. Dimova, R. Peterson, B. Mwashote, J. Chanton, W. Burnett. 2009. Extended time series measurements of submarine groundwater discharge tracers (^{222}Rn and CH_4) at a coastal site in Florida. Mar. Chem. 113: 137-147.

Sassen, R., I. MacDonald, N. Guinasso, S. Joye, A. Requejo, S. Sweet, J. Alcalá-Herrera, D. DeFreitas, D. Schink. 1998. Bacterial methane oxidation in sea-floor gas hydrate: significance to life in extreme environments. Geology 26:851-854.

Schütz, H., W. Seiler, R. Conrad. 1990. Influence of soil temperature on methane emission from rice paddy fields. Biogeochemistry. 11: 77-95.

Scranton, M., P. Brewer. 1977. Occurrence of methane in the near-surface waters of the western subtropical North-Atlantic. Deep-Sea Res. 24: 127-138.

Sebacher, D., R. Harriss, K. Bartlett, S. Sebacher, S. Grice. 1986. Atmospheric methane sources: Alaskan tundra bogs, an alpine fen and a subarctic boreal marsh. Tellus B 35B: 1-10.

Shah, S., S. Joye, J. Brandes, A. McNichol. 2013. Carbon isotopic evidence for microbial control of carbon supply to Orca Basin at the seawater-brine interface. Biogeosciences. 10:3175-3183.

Shalini, A., R. Ramesh, R. Purjava, J. Barnes. 2006. Spatial and temporal distribution of methane in an extensive shallow estuary, South India. J. Earth Syst. Sci. 115:451-460.

Shaw, T., W. Moore, J. Kloepfer, M. Sochaski. 1998. The flux of barium to the coastal waters of the southeastern USA: the importance of submarine groundwater discharge. Geochim. Cosmochim. Acta 62: 3047-3054.

Shim, MJ. 2011. Dissolved and colloidal element transport through the costal transition zone. Ph.D. thesis. Univ. of Southern Mississippi.

Sieburth, J. 1991. Methane and hydrogen sulfide in the pycnocline: a result of tight coupling of photosynthetic and "benthic" processes in stratified waters. Microbial

Production and Consumption of Greenhouse Gases: Methane, Nitrogen Oxides, and Halomethanes. American Society of Microbiology. 147-174.

Solomon, S., D. Qin, M. Manning, Z. Chen, M. Marquis, K.B. Averyt, M. Tignor, and H.L. Miller (eds.). 2007. Climate Change 2007: The Physical Science Basis. Contribution of Working Group I to the Fourth Assessment Report of the Intergovernmental Panel on Climate Change. Cambridge, UK, and New York, NY: Cambridge University Press.

Sowers, K. 2009. Methanogenesis. Encyclopedia of Microbiology (Third Edition). Academic Press. 265-286.

St Louis, V., C. Kelly, Ê. Duchemin, J. Rudd, D. Rosenberg. 2000. Reservoir Surfaces as Sources of Greenhouse Gases to the Atmosphere: A Global Estimate. BioScience. 50: 766-775.

Steele, S. Strode, K. Sudo, S. Szopa, G. van der Werf, A. Voulgarakis, M. van Weele, R. Weiss, J. Williams and G. Zeng. 2013. Three decades of global methane sources and sinks. Nature Geoscience.

Sweeney, C., E. Gloor, A. Jacobson, R. Key, G. McKinley, J. Sarmiento and R. Wanninkof. 2007. Constraining global air-sea gas exchange for CO_2 with recent bomb ^{14}C measurements. Global Biogeochem. Cycles 21: GB2015

Swinnerton, J., V. Linnenbom. 1967. Determination of the C_1 to C_4 hydrocarbons in sea water by gas chromatography. J. Chromatogr. Sci. 5: 570-573.

Thauer, R. 1998. Biochemistry of methanogenesis: a tribute to Marjory Stephenson: 1998 Marjory Stephenson Prize Lecture. Microbiology. 144:2377-2406.

Tilbrook, B., D. Karl. 1995. Methane sources, distributions and sinks from California
coastal waters to the oligotrophic North Pacific gyre. Mar. Chem. 49:51-64.

Topp, E., R. Hanson. 1991. Metabolism of radiatively important trace gases by methane-
oxidizing bacteria. Microbial production and consumption of greenhousegases:
methane, nitrogen oxides, and halomethanes. American Society for Microbiology,
Washington, DC. 71-90.

Upstill-Goddard, R., J. Barnes, T. Frost, S. Punshon, N. Owens. 2000. Methane in the
southern North Sea: Low-Salinity inputs, estuarine removal, and atmospheric
flux. Global Biogeochem. Cycles 14: 1205-1217.

U.S. Department of State. 2007. Projected Greenhouse Gas Emissions. In : Fourth
Climate Action Report to the UN Framework Convention on Climate Change.
U.S. Department of State, Washington, DC, USA.

Utsumi, M., Y. Nojiri. 1998. Oxidation of dissolved methane in a eutrophic, shallow lake:
Lake Kasumigaura, Japan. Limnol. Oceanogr. 43: 471-480.

Van der Nat, F.J., J. Middleburg. 2000. Methane emission from tidal freshwater marshes.
Biogeochemistry. 49: 103-121.

Wanninkof, R., W. Asher, D. Ho, C. Sweeney and W. McGillis. 2009. Advances in
Quantifying Air-Sea Gas Exchange and Environmental Forcing. Annu. Rev.:
Marine Sci. 1:213-244.

Warner, N., T. Kresse, P. Hays, A. Down, J. Karr, R. Jackson, A. Vengosh. 2013.
Geochemical and isotopic variations in shallow groundwater in areas of the
Fayetteville Shale development, north-central Arkansas. Applied Geochemistry.
35: 207-220.

Watanabe, S., N. Higashitani, N. Tsurushima, S. Tsunogai. 1995. Methane in the western North Pacific. J. Oceanogr. 51:39-60.

Wiesenburg, D., N. Guinasso Jr. 1979. Equilibrium Solubilities of Methane, Carbon Monoxide and Hydrogen in Water and Sea Water. J. Chem. Eng. Data 24: 356-360.

Wiesenburg, D., J. Brooks, B. Bernard. 1985. Biogenic hydrocarbon gases and sulfate reduction in the Orca Basin brine. Geochemi. Cosmochim. Acta 49: 2069-2080.

Yvon-Lewis, S., L. Hu, J. Kessler. 2011. Methane flux to the atmosphere from the Deepwater Horizon oil disaster. Geophys. Res. Lett. 38: L01602